Water Resources Research

RESEARCH ARTICLE

10.1029/2023WR036245

Effects of Short-Term Climate Variations on Young Water Fraction in a Small Pre-Alpine Catchment

C. Xia[1], G. Zuecco[2,3], C. Marchina[2], D. Penna[4,5], and M. Borga[2]

[1]School of Geography and Tourism, Chongqing Normal University, Chongqing, China, [2]Department of Land, Environment, Agriculture, and Forestry, University of Padova, Legnaro, Italy, [3]Department of Chemical Sciences, University of Padova, Padua, Italy, [4]Department of Agriculture, Food, Environment and Forestry, University of Florence, Florence, Italy, [5]Forest Engineering Resources and Management Department, Oregon State University, Corvallis, OR, USA

Key Points:

- The isotopic composition of water sources underwent a significant enrichment, likely due to the increasing air temperature
- Young water fractions (F_{yw}) varied between 0.16 and 0.64, and the estimates were sensitive to the sampling period and the fitting method
- Impacts of isotopic trends and sampling strategies should be considered in the selection and development of F_{yw} estimation methods

Supporting Information:

Supporting Information may be found in the online version of this article.

Correspondence to:

G. Zuecco,
giulia.zuecco@unipd.it

Citation:

Xia, C., Zuecco, G., Marchina, C., Penna, D., & Borga, M. (2024). Effects of short-term climate variations on young water fraction in a small pre-Alpine catchment. *Water Resources Research*, *60*, e2023WR036245. https://doi.org/10.1029/2023WR036245

Received 9 SEP 2023
Accepted 29 SEP 2024

Author Contributions:

Conceptualization: C. Xia, G. Zuecco, M. Borga
Data curation: G. Zuecco, C. Marchina
Formal analysis: C. Xia
Funding acquisition: G. Zuecco, D. Penna, M. Borga
Investigation: G. Zuecco, C. Marchina, D. Penna
Methodology: C. Xia, G. Zuecco
Project administration: M. Borga
Resources: G. Zuecco, C. Marchina
Supervision: M. Borga
Visualization: C. Xia, G. Zuecco
Writing – original draft: C. Xia, G. Zuecco

Abstract Continuous and extended observations of hydrometeorological parameters, alongside the analysis of the isotopic composition across diverse waters within catchments, can significantly enhance our understanding of the potential ramifications of climate change on the hydrological response. In this study, a comprehensive analysis of hydrometeorological and isotopic data was conducted over 10 hydrological years (October 2012–September 2022) within a small, forested catchment in the Italian pre-Alps, aiming to investigate the impacts of short-term climatic changes on the isotopic composition of waters and the young water fraction (F_{yw}). The results showed that the catchment experienced climate conditions with rapid warming and drying trends. Significant isotopic enrichments were observed in all sampled water sources, driven primarily by air temperature. F_{yw} was estimated to be 0.64 ± 0.06, 0.45 ± 0.07, and 0.16 ± 0.03 for stream water, soil water, and shallow groundwater based on the whole-period sinusoidal fittings, respectively. Comparative analyses comprising different approaches for the estimation of F_{yw} showed that time-windows scenarios and detrending corrections yielded smaller F_{yw} than approaches based on the whole-period fitting and discharge-sensitivity modeling. Such differences can be attributed to an uneven temporal distribution of stream water isotopic data, the difficulties in capturing high flows in a humid catchment characterized by a fast runoff response during rainfall-runoff events, and the presence of isotopic trends. Our findings underscore the imperative of integrating interannual isotopic trends and adopting appropriate sampling strategy and methodological approaches to ensure a robust F_{yw} estimation.

1. Introduction

Stable isotopes of hydrogen and oxygen are useful indicators for investigating runoff generation mechanisms, ecohydrological processes, and paleoclimatic fluctuations (Orlowski et al., 2023; Penna et al., 2018; Rozanski et al., 1992). Due to fractionation, the isotopic composition (δ^2H and δ^{18}O) of water sources strongly depends on local environmental factors such as air temperature, precipitation, and relative humidity (Dansgaard, 1964; Vystavna et al., 2021; Zhang & Wang, 2016). Due to rapid climatic variations currently occurring at the global scale, it is crucial to identify and investigate meteorological trends and their possible effects on the isotopic composition of different waters, which helps accurately interpret hydrological processes, assess water source origins, and predict potential impacts on ecosystems and water resource management. In catchments larger than 10 km^2, the spatial heterogeneity in land use, soil, and lithological characteristics and the combination of different hydrological processes can lead to difficulties in understanding isotopic responses to climate variations (Dutton et al., 2005; Rank et al., 2012; Reckerth et al., 2017). Conversely, small catchments (<10 km^2) are suitable areas to conduct high spatial resolution and long-term observations, and thus they can benefit from the study of temporal trends and the relation between isotopic composition and hydrometeorological variables (Penna, 2024; Penna & van Meerveld, 2019). Based on high-resolution isotopic observations over decadal scales, previous studies have reported clear isotopic trends associated with climate variations in precipitation in both global and regional scales. For example, 65 out of 98 GNIP (Global Network of Isotopes in Precipitation) sites present a significant increasing trend in δ^{18}O in precipitation under global warming (Wang & Chen, 2020), and 20 out of 28 sites show positive long-term δ^{18}O trends in precipitation in Germany under a nationwide trend of rising temperatures (Stumpp et al., 2014). However, except for precipitation, long time series (e.g., >5 years) of isotopic data of various waters, such as stream water and groundwater, are rarely reported.

10.1029/2023WR036245

Writing – review & editing: C. Xia, G. Zuecco, C. Marchina, D. Penna, M. Borga

Besides the usefulness of hydrogen and oxygen isotopes to investigate hydrological processes at the hillslope and small catchment scale, these tracers are widely used for the estimation of transit times (Benettin et al., 2022; Sprenger et al., 2019). Mean transit times (MTT) reflect the dynamics of water storage and release, which have been quantified in a variety of catchments under different climatic conditions (Barua et al., 2022; Rodgers et al., 2005; Soulsby et al., 2006; Xia et al., 2021). However, Kirchner (2016) pointed out that the MTT calculated using the sine wave method often exhibits significant uncertainties. Such uncertainties can reach several hundred percent when the sine wave method is applied to catchments with great spatial heterogeneity, due to the aggregation bias stemming from the pronounced nonlinearity in the relationship between tracer cycle amplitudes and MTT. Kirchner (2016) also showed that the metric called young water fraction (F_{yw}), defined as the fraction of stream water younger than 2–3 months, is not significantly affected by the aggregation bias and it can be used as an indicator of the typical hydrological behavior of a catchment (von Freyberg et al., 2018; Kirchner, 2016). F_{yw} can be estimated by computing the amplitude ratio of isotopic signals of stream water and precipitation (Kirchner, 2016). In recent studies, F_{yw} was estimated in catchments with different land use and climate, and the metric was positively correlated to the discharge and was influenced by multiple factors including elevation, duration of the snow cover and low flow, soil temperature, soil moisture, land use, precipitation amount, and vegetation cover (Ceperley et al., 2020; von Freyberg et al., 2018; Gentile et al., 2023; Song et al., 2017; Trinh et al., 2020). In the estimation of F_{yw}, the sources of uncertainty have also been explored. Generally, the isotopic composition of precipitation in a mid-latitude catchment follows an approximate seasonal pattern and the periodicity is propagated into the other waters to form a certain runoff regime. This hypothesis forms the basis for estimating the F_{yw}. In catchments with a great variability in discharge, low sampling frequency and non-weighted fitting method resulted in the underestimation of F_{yw} (Gallart, Valiente, et al., 2020). Indeed, the selection of the sampling and calculation period could lead to a marked uncertainty in the F_{yw} estimation, particularly for short-term data sets (Stockinger et al., 2019). For instance, extreme events (e.g., heat waves) and intermittent flow in dry periods can decrease the reliability of the F_{yw} estimation (Bansah & Ali, 2019; Stockinger et al., 2019). Furthermore, the isotopic composition of different waters not only varies at the event and at the seasonal scale, but it may also exhibit interannual difference in fluctuation patterns and long-term trends due to climate variations. Such differences and trends change the variability and transmission dynamics of isotopes within water systems, thereby diminishing the fitting accuracy of the fixed periodic function, which is a potential source of uncertainty for tracer-aided F_{yw} estimation. Since F_{yw} is a highly discharge-sensitive metric, capturing the isotopic information under different flow regimes (e.g., baseflow or high flow periods) is necessary to guarantee the accuracy of estimation, and it requires high temporal resolution and long-term observations in catchments (Xia et al., 2023). Stockinger and Stumpp (2024) proved that the involvement of long-term data and the calculation of time-variable F_{yw} (i.e., based on time windows) could promote the inter-catchment comparability and improve the understanding of sources of uncertainties. However, despite the possible sensitivity of F_{yw} to changes in the isotopic composition of different waters due to climate trends, and the necessity of exploiting long-term isotopic data, in most published papers focusing on F_{yw}, the observation period is not long enough (for most cases less than 5 years) to reflect the influence of isotopic trends caused by climate variations on the sinusoidal fit (Burt et al., 2023; Jasechko et al., 2016; Stockinger et al., 2019). Generally, climate change refers to significant changes or prolonged alterations in the statistical properties of the average climate over a considerable period, typically 30 years or longer. Considering that isotopic data sets of multiple waters spanning over 30 years or more are scarce, in this study, we examine and define the climate changes within the range of 5–15 years as "short-term climate variations" and focus on their impact on isotopic variations. In this work we exploit isotopic data collected in 10 hydrological years in a small pre-Alpine catchment to better understand the isotopic response to short-term climate variations and the implications for the F_{yw} estimation. In particular, we address the following specific questions:

1. What is the temporal variability in the main hydrometeorological variables (i.e., precipitation, discharge, and soil moisture)?
2. What is the temporal variability in the isotopic composition of different water sources and how does it relate with air temperature and precipitation amount?
3. How do short-term climate variations and methodological approaches impact on F_{yw} estimation at the small catchment scale?

2. Materials and Methods

2.1. Study Area

Ressi is an experimental catchment located in the Italian pre-Alps (45.79°N, 11.27°E, shown in Figure 1; Zuecco et al., 2021). It is a small sub-catchment of the 116-km^2 Posina basin, covering an area of 0.024 km^2. The catchment belongs to a humid temperate climate zone. The elevation of the catchment ranges from 598 to 721 m, and the average slope is 31° (Zuecco et al., 2021). A stream flows from southeast to northwest along a 150-m channel. On each side of the stream, there is a small riparian zone bordered by steep hillslopes. The catchment is almost completely covered by a dense deciduous forest, and the geology consists of a sequence of rhyolites and dacites from Triassic volcanic lithologies.

2.2. Field Observations and Isotopic Analysis

The hydrometeorological monitoring of the Ressi catchment started in August 2012 (Zuecco et al., 2021). Precipitation was recorded at 5- or 10-min interval by a weather station located in the northeast part of the catchment, whereas air temperature was recorded at 5-min interval starting from 2018. Precipitation and air temperature were also monitored at three meteorological stations, that is, Passo Xomo (1,051 m a.s.l.), Contrà Doppio (734 m a.s.l.), and Castana (420 m a.s.l.) maintained by the Agency for Environmental Protection of Veneto Region (ARPAV). They are located at a 2.3–4.8 km distance from the Ressi catchment, and data from these three stations are used for filling the data gaps in the Ressi precipitation time series. Given that air temperature in Ressi covered a short period (2018–2022), in this study we used temperature data recorded at hourly timescale in Contrà Doppio (weather station with an elevation similar to Ressi). Stream water level was measured at a 5-min resolution at the outlet of the catchment by a pressure transducer installed behind a V-notch weir (Zuecco et al., 2021). Soil moisture within the near-surface layer (0–30 cm) was monitored at a 10-min interval employing four reflectometers (CS625, Campbell Scientific Inc., USA). These reflectometers were strategically situated at distinct locations along a transect: SM1 was positioned within the riparian zone, at a distance of approximately 1 m from the stream; SM2 was situated at the interface between the riparian zone and the hillslope; SM3 was located in the middle section of the hillslope, while SM4 was placed in the uppermost section of the hillslope. In 2021, SM4 was removed due to maintenance issues, and SM5 was installed 5 m away from SM4 (Figure 1). Depths to the water table were recorded by six piezometers (four in the riparian zone and two in the hillslope) with a 5-min interval. In this study, we used data collected from the riparian piezometer with the longest time series (Gelmini et al., 2022, Figure 1).

Precipitation, stream water, shallow groundwater, and soil water samples were collected at approximately monthly timescale and during selected rainfall-runoff events for isotopic analysis. In this work, we considered the isotopic data set collected between October 2012 and September 2022. For precipitation, we considered only bulk samples retrieved approximately monthly, using 5-l high-density polyethylene bottles equipped with a funnel and a layer of mineral oil to prevent evaporation (Marchina et al., 2020). Stream water was collected manually (with grab samples) during baseflow conditions at approximately monthly resolution, and by an automatic water sampler during selected rainfall-runoff events at about 30-min or hourly temporal resolution (grab samples were collected every 5–15 min during some summer storms). Shallow groundwater and soil water were retrieved manually at a piezometer and by a suction lysimeter in the riparian zone, respectively. Groundwater and soil water were collected monthly or with a (sub-) daily resolution during the selected rainfall-runoff events. In total, 116 precipitation samples, 1,358 stream water samples (collected over 602 days), 248 shallow groundwater samples (collected over 237 days) and 161 soil water samples (collected over 151 days) were collected during the 10-year observation period. All water samples were stored in 50-ml high-density polyethylene bottles in a fridge at 4°C, until the isotopic analysis. The isotopic composition (δ^2H and δ^{18}O) of the samples was determined by a DLT-100 analyzer (Los Gatos Research Inc. USA), based on the off-axis integrated cavity output spectroscopy method. Memory effect (i.e., carry-over effect) on isotopic measurements was minimized following the procedure described in Penna et al. (2012). Isotopic composition is expressed as part per mil deviation (δ value) from Vienna Standard Mean Ocean Water (VSMOW). The uncertainties of measurements for δ^2H and δ^{18}O are 1.0 and 0.20‰, respectively (Marchina et al., 2020).

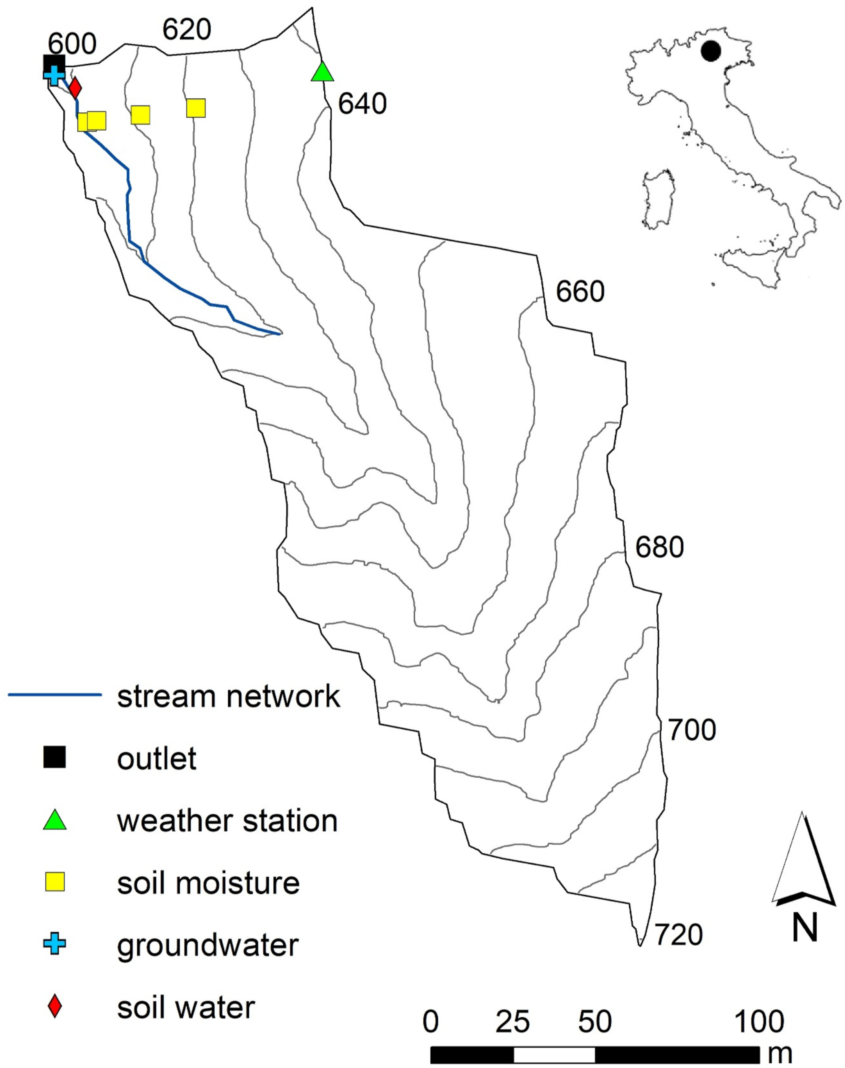

Figure 1. Geographic location of the Ressi catchment and of the instrumentation used for this study. In the legend, "groundwater" indicates the location of the piezometer used in this study for the shallow groundwater sampling. Only four locations are displayed for five soil moisture probes (from SM1 to SM5) because SM5 was installed very close to (i.e., 5 m away from) SM4.

2.3. Analysis of the Temporal Variability in Hydrometeorological and Isotopic Data

Mann-Kendall test was used to analyze the temporal variability (i.e., trends) of hydrometeorological and isotopic data in the Ressi catchment. Mann-Kendall test is a non-parametric test that can be used to effectively distinguish whether the time series of hydrometeorological variables have a definite variation trend without considering the assumption of normality (Hamed & Ramachandra Rao, 1998; Kahya & Kalayci, 2004). Assuming a sequential data set that contains n samples as X_T (x_1, x_2, x_3, …, x_n), the Mann-Kendall parameter S is defined as follows:

$$S = \sum_{i=2}^{n} \sum_{j}^{i-1} \text{sign}(x_j - x_i) \tag{1}$$

The "sign ()" is a discrimination function that is defined as follows:

$$\operatorname{sign}(x_j - x_i) = \begin{cases} 1, & (x_j - x_i) > 0 \\ 0, & (x_j - x_i) = 0 \\ -1, & (x_j - x_i) < 0 \end{cases} \tag{2}$$

The standard normal statistic z of Mann-Kendall test is calculated as follows:

$$z = \begin{cases} \frac{S-1}{\sqrt{n(n-1)(2n+5)/18}}, & S > 0 \\ 0, & S = 0 \\ \frac{S+1}{\sqrt{n(n-1)(2n+5)/18}}, & S < 0 \end{cases} \tag{3}$$

In the equation, a positive z value represents an upward temporal trend, and a negative z value represents a downward one. Trends were considered significant when $p < 0.05$.

Theil-Sen's estimator is a robust method for estimating the slope of a linear relationship between two variables (Sen, 1968). When using this method to identify the data variation with time, slopes will be computed for all the pairs of ordinal time points and then the median of them will be used as an estimate of the overall slope (i.e., Sen's slope). The results obtained by Theil-Sen's estimator are insensitive to outliers, so this method is more accurate and robust than the least square method for skewed distributions and heteroscedastic data. Therefore, Sen's slope was used for quantifying the degree of trends for hydrometeorological and isotopic time series.

Autocorrelation is present when data points in a time series are systematically correlated with other data points in the same time series but at different points of time. Hydrological time series showing seasonal or daily patterns are in most cases significantly autocorrelated. To perform the Mann-Kendall test, the original data sequence should be non-autocorrelated; indeed, the autocorrelation of observed data can amplify the significance of data series trends, leading to unrealistic results (Cox & Stuart, 1955; Yue & Wang, 2002; Zwiers & Von Storch, 1995). For a better assessment of temporal trend in hydrometeorological and isotopic data, a trend-free pre-whitening method is adopted to remove the influence of autocorrelation (Yue et al., 2002).

First, the linear trend is calculated for the initial time-series data set X_T $(x_1, x_2, x_3, \ldots, x_n)$ by Sen's slope:

$$\beta = \text{Median}\left(\frac{x_j - x_i}{j - i}\right), \forall i < j \tag{4}$$

where β is the Sen's slope for the initial time series, the symbol "∀" means "for all" and i and j represent the time (month or day) when the data are collected. Second, the trend is removed and a new sequence Y_T $(y_1, y_2, y_3, \ldots, y_n)$ without trend is generated:

$$y_t = x_t - T_t = x_t - \beta t \tag{5}$$

where t means the time of each measured data, and T_t represents the trend item, and n means the length of the time series. Third, the lag-1 autocorrelation coefficient (r_1) is calculated and removed to obtain the residual sequence Y_T' (y_1', y_2', y_3', …, y_n'):

$$y_t' = y_t - r_1 y_{t-1} \tag{6}$$

The equation for the calculation of r_1 is as follows:

$$r_1 = \frac{\sum_{t=1}^{n-1} (y_t - \bar{y})(y_{t+1} - \bar{y})}{\sum_{t=1}^{n} (y_t - \bar{y})^2} \tag{7}$$

where $\bar{y}$ means the average value of the time-sequence Y_T. Last, the trend item (T_t) is blended with the residual sequence Y_T' and the new series $Y_T''(y_1'', y_2'', y_3'', \ldots, y_n'')$, no longer influenced by effects of autocorrelation, is obtained:

$$y_t'' = y_t' + T_t = y_t' + \beta t \tag{8}$$

Although having time series data with equal intervals is not a requirement for Mann-Kendall test, this is an essential condition for the determination of Sen's slope. Therefore, for trend analysis, interpolation was performed by cubic polynomial method based on measured isotopic values to generate equal intervals in the isotopic composition of the water sources. For isotopic data in stream water, volume-weighted average at daily timescales were calculated. For isotopic data in groundwater and soil water, daily mean values (arithmetic averages) were computed for days with multiple samples. Relative slopes for hydrometeorological factors and isotopes were also calculated as the ratios of the Sen's slopes and the mean values of time series and were standardized as "%/10yr." The trend-free pre-whitening Mann-Kendall test and Sen's slope trend were performed by using MATLAB 2020a software.

To compare the variability of hydrometeorological and isotopic factors, the coefficient of variation (CV) was calculated as the ratio of the standard deviation to the mean value.

2.4. Estimation of F_{yw}

The F_{yw} for different waters was calculated following the method proposed by Kirchner (2016). Theoretically, the transit-time distribution $h(\tau)$ was assumed to belong to the family of gamma distributions. The time series of isotopic signals in precipitation was considered as input water in this model. The variation of isotopic signals in water sources (i.e., stream water, soil water, and groundwater), considered as output waters of the catchment, was regarded as the convolution of transit time distribution with signals in precipitation.

Following Ceperley et al. (2020), sine wave fitting was performed by Levenberg–Marquardt algorithm to fit the isotopic signals in precipitation and other waters, respectively, following Equations 9 and 10 below:

$$C_p(t) = Ap \sin\left(2\pi f t - \varphi_p\right) + k_p \tag{9}$$

$$C_s(t) = As \sin\left(2\pi f t - \varphi_s\right) + k_s \tag{10}$$

where t is the time, $C_p(t)$ and $C_s(t)$ represent the isotopic time series in precipitation and other water sources, respectively. Ap and As are amplitudes of sine waves fitted to isotopic signals in precipitation and other waters, f is the frequency of annual isotopic fluctuation (f is set as 1/365.25 in calculation based on 1-day steps), and k is the vertical shift of the sine wave. The uncertainties of As and Ap were represented by the standard errors of the sine wave fitting. The adjusted coefficient of determination (adjusted R^2 value) was used to evaluate the goodness of fit of the sine wave to the time series of isotopic data. For precipitation, isotopic values of bulk samples were used for fitting, and the associated precipitation amount was used as weight and assigned to the sampling dates of each collection period. For stream water, soil water, and groundwater, isotopic values for grab samples were used for the fitting. The discharge was used as weight and assigned to the sampling time for stream water, while an unweighted approach was used for fitting the sine wave to the isotopic composition of soil water and groundwater. MATLAB scripts published by Ceperley et al. (2020) were used for the sine wave fitting.

As proved by Kirchner (2016), the F_{yw} of waters can be estimated approximately by the "amplitude ratio approach":

$$\mathrm{Fyw} = \frac{As}{Ap} \tag{11}$$

The uncertainty of the estimated F_{yw} was determined based on the standard errors of As and Ap, following the Gaussian error propagation, as shown in Equation 12:

$$\sigma_{\mathrm{Fyw}} = \sqrt{\left(\frac{\partial \mathrm{Fyw}}{\partial As}\sigma_{As}\right)^2 + \left(\frac{\partial \mathrm{Fyw}}{\partial Ap}\sigma_{Ap}\right)^2} \tag{12}$$

where σ_{Fyw} means the uncertainty of $\mathrm{F_{yw}}$, $\frac{\partial \mathrm{Fyw}}{\partial As}$ and $\frac{\partial \mathrm{Fyw}}{\partial Ap}$ indicate the partial derivatives of Equation 11 with respect to variables As and Ap, and σ_{As} and σ_{Ap} mean the uncertainties of As and Ap, respectively.

Besides the whole-period sine wave fitting applied to the original time series, we used alternative approaches for the aggregation of the isotopic data and the consequent sine wave fitting.

1. *Time-variable F_{yw} based on moving time windows*. Based on the monthly isotopic composition of precipitation and stream water within 120 months, the method of moving time windows was employed to capture and compare the isotopic signals within different sub-periods, and thus obtain the time-variable $\mathrm{F_{yw}}$ values. In previous studies, Stockinger et al. (2019) employed 1-year time windows with 1-week and 4-week timesteps for $\mathrm{F_{yw}}$ estimation based on 4.5-year isotopic data; Stockinger and Stumpp (2024) employed 1-year to 8-year time windows with monthly timesteps for $\mathrm{F_{yw}}$ estimation based on 15-year isotopic data in 9 mid-European rivers. The selection of time windows for time-variable $\mathrm{F_{yw}}$ estimation should be performed considering both the length of observation period and the temporal density of samples. Accordingly, time windows with three different sizes and timesteps with two different lengths were adopted for calculation in the Ressi catchment, including (a) 1-year time windows with biweekly timesteps (235 individual $\mathrm{F_{yw}}$ results obtained); (b) 1-year time windows with monthly timesteps (109 individual $\mathrm{F_{yw}}$ results obtained); (c) 2-year time windows with biweekly timesteps (209 individual $\mathrm{F_{yw}}$ results obtained); (d) 2-year time windows with monthly timesteps (97 individual $\mathrm{F_{yw}}$ results obtained); (e) 3-year time windows with biweekly timesteps (183 individual $\mathrm{F_{yw}}$ results obtained); (f) 3-year time windows with monthly timesteps (85 individual $\mathrm{F_{yw}}$ results obtained). The flow-weighted averages were calculated for time window-based $\mathrm{F_{yw}}$ estimates to represent the overall feature of the whole observation period.
2. *F_{yw} estimation after a detrending correction*. The uncertainty of fitting results may strongly increase when employing fixed periodic functions in instances where significant trends are present within the isotopic data sets of precipitation and stream water (as well as other waters). The fundamental theory for $\mathrm{F_{yw}}$ estimation was set upon the hypothesis that isotopic variation in precipitation presents a periodic regime and the periodicity transmits to that in other waters, without including the possible temporal isotopic trends. Therefore, a detrending method was proposed based on the following premises: (a) We assume that climate change induces linear trends in the isotopic signals of precipitation and stream water; (b) We disregard the interdependency between isotopic trends in precipitation and those in stream water. Such method is not intended to work as an efficient approach for enhancing $\mathrm{F_{yw}}$ estimation accuracy, but rather to elucidate the impacts of isotopic trends on $\mathrm{F_{yw}}$ estimation. The linear detrending method was applied as follows:
    1. The isotopic increase of each sampling date was calculated by the following equation:

$$\Delta\delta^{18}\mathrm{O} = \Delta\mathrm{T} \times \text{Sen's slope} \tag{13}$$

    where 1 October 2012 was set as initial time (T_0), and ΔT means the time span from T_0;
    2. The $\Delta\delta^{18}$O was subtracted by the measured δ^{18}O values to obtain the corrected $\delta^{18}\mathrm{O_c}$ by the following equation:

$$\delta^{18}\mathrm{O}_c = \delta^{18}\mathrm{O} - \Delta\delta^{18}\mathrm{O} \tag{14}$$

    3. The sinusoidal curve was fitted to the whole period using the corrected $\delta^{18}\mathrm{O_c}$ to obtain the corrected amplitudes of precipitation (Ap) and stream water (As).
    The corrected $\mathrm{F_{yw}}$ was calculated using the ratio between the corrected As and Ap.
3. *Simulated discharge-sensitive F_{yw}*. The nonlinear fitting method proposed by Gallart, von Freyberg, et al. (2020), which is based on the dependence of the $\mathrm{F_{yw}}$ on stream discharge, was employed to obtain the discharge-sensitive $\mathrm{F_{yw}}$. After identifying different flow regimes represented by the percentile of flow

Table 1
Explanation Table for F_{yw} Symbols Obtained by Different Computation Methods

Symbol for F_{yw}	Description of the computation methods
F_{yw0}	F_{yw} calculated by the initial whole-period fitting method
F_{ywt}(s-bw/m)	Time-variable F_{yw} computed by moving time windows
F_{ywt}*(s-bw/m)	Time-variable F_{yw} computed by moving time windows where windows with low R^2 values were removed
F_{ywc}	F_{yw} computed after linear detrending correction based on whole period data
$F_{yw}(Q)$	F_{yw} simulated by integrating its discharge sensitivity over the entire 5-min discharge record

Note. s means the size of time window (1, 2 or 3 years), *bw/m* means the length of timestep, which is biweekly (*bw*) or monthly (*m*).

duration curve, an exponential function was used for fitting the relation between F_{yw} and the median discharges of selected regimes as follows:

$$F_{yw}(Q) = 1 - (1 - F_0)\exp(-QS_d) \tag{15}$$

where F_0 represents the virtual F_{yw} for $Q = 0$ and S_d with a unit of Q^{-1} is the discharge sensitivity metric. By splitting the flow duration curve (shown in Figures S1a and S1b of Supporting Information S1) into 20 equal parts (each representing the discharge in a range of 5%), the median discharge value in each range was calculated. The *As* for each 5% range can be obtained by fitting the sine function curve with the stream water isotopes contained in each part and the corresponding sampling time, and thus the F_{yw} value can be obtained through the amplitude ratio method. The relation between the median discharge and F_{yw} can be established by following the method by Gallart, von Freyberg, et al. (2020). Then, the discharge-sensitive F_{yw} could be modeled based on the obtained F_0 and S_d values and the observed whole-period discharge data. In the Ressi catchment, 1,358 isotope/discharge values in stream water were used for obtaining the metrics of Equation 15, and 1,014,120 monitored 5-min discharge was used for simulating the F_{yw} (Q) during the 10-year observation period. The flow-averaging of the simulated $F_{yw}(Q)$ was regarded as a flow-weighted F_{yw} covering all flow records.

As multiple approaches were used to estimate F_{yw}, the expressions of this metric by different methods are clarified in Table 1 to perform a clear comparison in the results and discussion sections.

3. Results

3.1. Temporal Variability in the Hydrometeorological Data

The mean annual temperature and annual precipitation recorded at the three ARPAV weather stations (i.e., Passo Xomo, Contrà Doppio and Castana) from January 1994 to December 2022 are shown in Figure 2. For precipitation (Figure 2a), the amounts and variations were similar between the three stations. The maximum annual precipitation was 3,444 mm observed at Passo Xomo in 2002, while the minimum was 993 mm observed at Castana in 2022. The average annual precipitation amounts are 2,008 mm, 1,894 mm, and 1,802 mm for Passo Xomo, Contrà Doppio and Castana, respectively. For mean air temperature, the values were similar between Contrà Doppio and Castana, but they were much lower in Passo Xomo, due to the difference in elevation. The patterns of temperature variation were similar for all stations. Except for seasonal fluctuation, air temperature also showed great interannual variations. The highest annual mean temperature of 11.0°C was observed at Contrà Doppio in 2022, while the lowest one of 6.5°C was recorded at Passo Xomo in 1996. The average temperatures for 29 years were 8.2°C, 9.7°C and 9.8°C for Passo Xomo, Contrà Doppio and Castana, respectively.

Daily mean temperature (monitored in Contrà Doppio) and precipitation in the Ressi catchment from October 2012 to September 2022 are shown in Figure 3a. During the observation period of 10 hydrological years, the average temperature (from Contrà Doppio station) was 10.1°C and the average annual precipitation was 2,115 mm. Both temperature and precipitation amount were higher than long-term averages at adjacent stations, showing that the

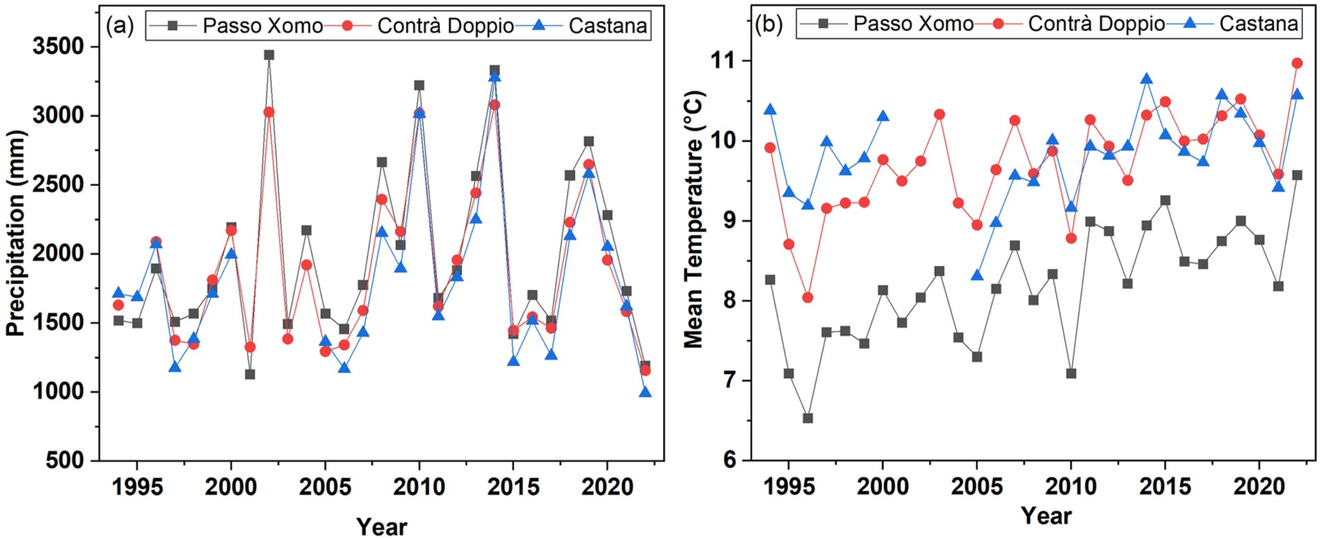

Figure 2. Time series of (a) annual precipitation and (b) mean annual air temperature (period 1994–2022) at three ARPAV weather stations located close to Ressi.

climate condition was relatively wetter and warmer during our observation period. Temperature and precipitation had clear seasonal variations. Generally, precipitation amount was high in spring and late autumn, with most peaks occurring in November, while dry periods were typical in winter, summer, and early autumn.

The seasonal variation in precipitation was reflected in discharge and soil moisture (Figures 3b and 3c). Based on monthly records (cumulative precipitation and averages for other metrics), the correlation coefficients (Pearson's r) were significant at 0.01 confidence level between time series of precipitation, soil moisture, and discharge. Among the soil moisture data, those from SM5 was not used for correlation analysis due to the short monitoring period. Precipitation presents the strongest positive correlation with mean discharge ($r = 0.83$), followed by the mean soil moisture in the upper part (SM4, $r = 0.44$), toe (SM2, $r = 0.39$) and middle part (SM3, $r = 0.38$) of the hillslope, and it presents the weakest correlation with soil moisture in the riparian zone (SM1, $r = 0.35$). The average soil moisture detected at four locations (by probes SM1, SM2, SM3 and SM4) were 27.6%, 29.7%, 14.2% and 15.4%, respectively. Soil moisture was much higher in the riparian zone and toe of the hillslope than in the middle and upper parts of the hillslope. The highest soil moisture values were generally observed in November during large rainfall-runoff events. Discharge showed a similar temporal behavior and had a positive correlation (average $r = 0.50$) with soil moisture. The monthly mean discharges ranged between 0.18 and 20.95 mm/d, with an average of 2.85 mm/d, showing a marked seasonal and interannual variability. High discharges were observed in October and November and in spring (from March to May) in most hydrologic years (Figure 3 and Figure S1c in Supporting Information S1). The order of CV in the variables was discharge (2.62) > precipitation (0.82) > soil moisture measured by SM4 (0.18) = soil moisture by SM3 (0.18) > soil moisture by SM2 (0.17) > soil moisture measured by SM1 (0.10).

Results from the pre-whitening Mann-Kendall test indicate that both temperature and precipitation presented upward trends (although some were not significant) for long-term monthly records from January 1994 to December 2022 at the three ARPAV weather stations (Table 2). During the short-term observation period from October 2012 to September 2022, the temperature showed upward trends, while precipitation showed downward trends, but these trends were not significant. According to the relative slopes (Table 2), the temperature increase was much more rapid during 2012–2022, with a mean rate of 15.1%/10yr for the three ARPAV weather stations compared with that of the long-term period (4.4%/10yr). Precipitation amount during the 2012–2022 period showed a negative trend compared to that during the long-term period (Table 2). According to the relative slopes, the absolute values of descending rate (average = −3.43%/10yr) were much higher during the 2012–2022 period compared with the increasing rate of long-term variations (average = 0.42%/10yr).

According to the measured data in the Ressi catchment, downward trends were found for precipitation, discharge, and soil moisture on a monthly scale (pre-whitening Mann-Kendall test, Table 3). Among these variables, the trends for discharge and soil moisture were significant at 0.05 confidence level ($|z| > 1.96$). An upward trend was

10.1029/2023WR036245

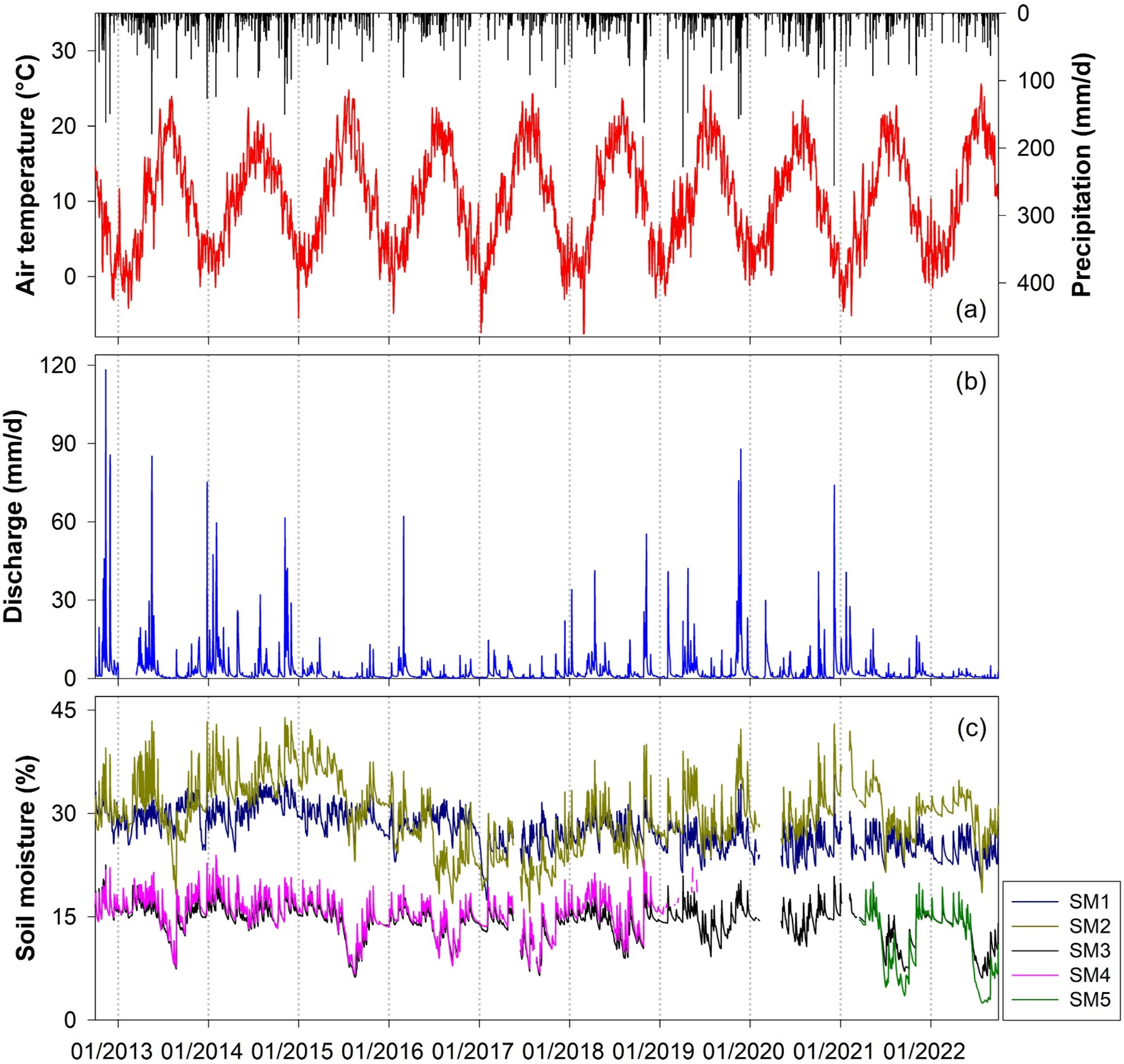

Figure 3. Time series of daily hydrometeorological variables in the Ressi catchment in the period October 2012–September 2022. (a) Air temperature (Contrà Doppio) and precipitation, (b) discharge at the catchment outlet and (c) soil moisture in five locations (from SM1 to SM5).

Table 2
Sen's Slopes and Relative Slopes for Long-Term (January 1994–December 2022) and Short-Term (October 2012–September 2022) Monthly Meteorological Data (Asterisks Mean the Results Are Significant at 0.05 Confidence Level Identified by Pre-Whitening Mann-Kendall Test)

		January 1994–December 2022				October 2012–September 2022			
	Station	Temperature	Z value	Precipitation	Z value	Temperature	Z value	Precipitation	Z value
Sen's slope	Passo Xomo	0.056°C/yr*	2.39	1.38 mm/yr*	2.02	0.16°C/yr	1.24	−6.69 mm/yr	−1.83
	Contrà Doppio	0.045°C/yr	1.82	0.65 mm/yr	1.06	0.16°C/yr	1.33	−7.87 mm/yr*	−2.43
	Castana	0.017°C/yr	0.62	0.35 mm/yr	0.52	0.11°C/yr	0.89	−6.46 mm/yr*	−1.98
Relative slope (%/10yr)	Passo Xomo	6.89*	/	0.70*	/	18.4	/	−3.1	/
	Contrà Doppio	4.58	/	0.35	/	15.9	/	−3.9*	/
	Castana	1.74	/	0.22	/	11.0	/	−3.3*	/

Note. Sen's slope values are reported in °C/yr and mm/yr.

Table 3
Sen's Slopes and Relative Slopes for Short-Term (October 2012–September 2022) Monthly Hydrometeorological Records in the Ressi Catchment (Double and Single Asterisks Mean the Results Are Significant at 0.01 and 0.05 Confidence Level, Respectively, Identified by Pre-Whitening Mann-Kendall Test)

Variable	Z value	Sen's slope	Relative slope
Temperature (Contrà Doppio)	1.33	0.16°C/yr	15.9%/10yr
Precipitation	−1.78	−6.38 mm/yr	−3.0%/10yr
Discharge	−2.45*	−0.11 mmd^{-1}/yr*	−39.6%/10yr*
Soil moisture (riparian)	−9.72**	−0.67%/yr**	−24.4%/10yr**
Soil moisture (toe of hillslope)	−3.41**	−0.29%/yr**	−10.0%/10yr**
Soil moisture (middle hillslope)	−4.22**	−0.24%/yr**	−16.8%/10yr**

Note. Sen's slope values are reported at the annual scale.

observed for temperature according to the records in Contrà Doppio, with a relative slope of 15.9%/10yr. The relative slope for precipitation decrease was −3.0%/10yr. Among all variables, the most extreme relative slope (−39.6%/10yr) was observed for discharge. For soil moisture, the relative decreasing rate was faster in the riparian zone than in the toe and middle part of the hillslope.

3.2. Temporal Variability in the Isotopic Composition of Different Water Sources

According to the 10 hydrological year records, δ^{18}O varied between −15.55‰ and −1.75‰ (average: −8.50‰) in precipitation, −11.25‰ and −4.44‰ (average: −8.38‰) in stream water, −12.19‰ and −5.19‰ (average: −8.25‰) in soil water, and −11.21‰ and −6.16‰ (average: −8.74‰) in shallow groundwater. Generally, the monthly average δ^{18}O values varied seasonally in precipitation and stream water, with more positive values occurring in summer and more negative occurring in winter, while the seasonal isotopic variation in shallow groundwater and soil water was much weaker (Figure 4). In the period October 2014–September 2015, no clear minimum in δ^{18}O was observed in stream water, although the seasonality in the isotopic composition of precipitation was marked. Compared to the other water sources, the monthly variation in the isotopic composition of shallow groundwater was more dampened. The δ^{18}O variation pattern in groundwater was different from those in other water sources, and the variability was particularly weak over an extended period spanning from July 2014 to September 2018. The lowest CV of 0.08 was observed for δ^{18}O in groundwater, followed by that in stream water (0.13) and soil water (0.17). The highest CV for δ^{18}O was 0.31 and it was observed in precipitation.

The δ^2H–δ^{18}O relation for precipitation and other waters is plotted in Figure 5 and the parameters for the regression lines are reported in Table 4. The local meteoric water line (LMWL, $\delta^2\text{H} = (7.72 \pm 0.13)\,\delta^{18}\text{O} + (11.25 \pm 1.12)$) presented similar slope and intercept with those of the global meteoric water line (GMWL, $\delta^2\text{H} = 8\delta^{18}\text{O} + 10$) proposed by Craig (1961), reflecting that the overall meteorological conditions during our observation period were close to the global average. The slope of the stream water line (SWL) was significantly lower than that of LMWL ($p < 0.01$). The soil water line (SLWL) had a slope similar to that of SWL (Table 4), while the parameters were significantly different from those of the groundwater line (GWL, $p < 0.001$). GWL had a much lower slope and intercept compared with the other lines, and the coefficient of determination (R^2 value) of regression was 0.68, which is smaller than that of the other waters (Table 4). Despite these differences in the regression lines, most of stream water, soil water and groundwater samples plotted within the 95% prediction interval of the LMWL (Figure 5b), suggesting that few samples may have occasionally experienced isotopic fractionation.

As shown in Table 5, δ^{18}O was characterized by significant positive trends at 0.01 confidence level ($|z| > 2.576$) for precipitation, stream water, soil water, and groundwater in Ressi, which were consistent with the trend for temperature, but in contrast with those for factors related to wetness. The Sen's slope and relative slope of δ^{18}O showed the same order of soil water (0.208‰/yr, 23.9%/10yr) > precipitation (0.161‰/yr, 17.9%/10yr) > groundwater (0.111‰/yr, 10.4%/10yr) > stream water (0.075‰/yr, 8.7%/10yr).

To identify the meteorological factor controlling the isotopic variation in precipitation, linear regressions for 10 hydrological years were performed between monthly mean δ^{18}O and local meteorological parameters (i.e., mean temperature and precipitation amount) (Figure 6 and Table S1 in Supporting Information S1). For the whole

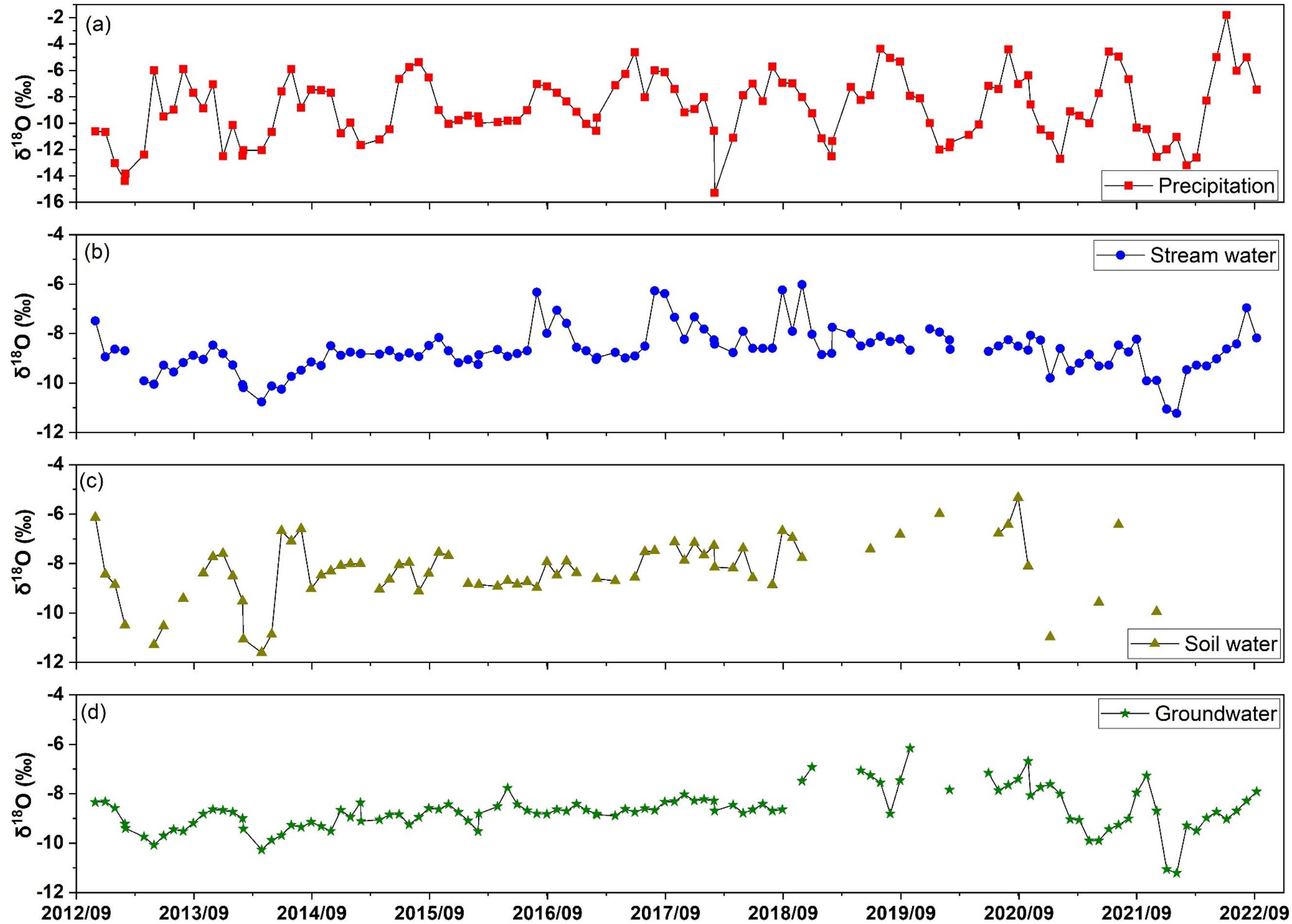

Figure 4. Time series of monthly mean $\delta^{18}O$ in (a) precipitation, (b) stream water, (c) soil water and (d) groundwater in the Ressi catchment from October 2012 to September 2022. Volume-weighted mean values are used for precipitation and stream water, whereas arithmetic mean values are used for soil water and groundwater.

period, $\delta^{18}O$ showed a significant positive correlation ($r = 0.81$) with air temperature at the 0.01 confidence level, and there was a non-significant negative correlation ($r = -0.08$) with precipitation amount. As shown in Table S1 of Supporting Information S1, $\delta^{18}O$ of precipitation always showed significant positive relations with air temperature at the 0.05 confidence level for all hydrological years, with a slope ranging from 0.14 ± 0.04 (2015–2016) to 0.49 ± 0.08 (2021–2022) and an intercept ranging from −13.98 ± 0.94 (2021–2022) to −9.91 ± 0.67 (2016–2017), while $\delta^{18}O$ presented non-significant relations with precipitation amount for all hydrological years, with low R^2 values, varying from 0.01 to 0.29. The similar positive trends (shown in Tables 3 and 5) and significant positive $\delta^{18}O$-Temperature relations (Figure 6 and Table S1 in Supporting Information S1) suggested that air temperature increase was a potential driving factor of the increasing isotopic trend in the Ressi catchment. The slope and intercept of $\delta^{18}O$-Temperature regression for the whole period were 0.33 and −12.20, respectively.

3.3. F_{yw} Estimation for Different Waters

Based on measured $\delta^{18}O$ data in precipitation, stream water, soil water, and groundwater, the sinusoidal regressions from Equations 9 and 10 were employed to fit the 10-year time series of isotopic signals (Figure 7). The adjusted R^2 values of sinusoidal fitting were 0.51 and 0.48 for $\delta^{18}O$ in precipitation and stream water, respectively, and those in soil water and groundwater were 0.31 and 0.16, respectively. The contrasting goodness of fit reflected the different seasonal variability in the isotopic composition of the water sources. The observed time series of $\delta^{18}O$ in soil water and shallow groundwater (Figure 4) and the low R^2 values (Figure 7) indicated a very weak seasonal periodicity in these waters. The amplitudes of $\delta^{18}O$ in precipitation (*Ap*), stream water (*As*), soil water (*Asl*), and groundwater (*Ag*) were 2.59 ± 0.24‰ (standard error), 1.67 ± 0.06‰, 1.17 ± 0.14‰ and

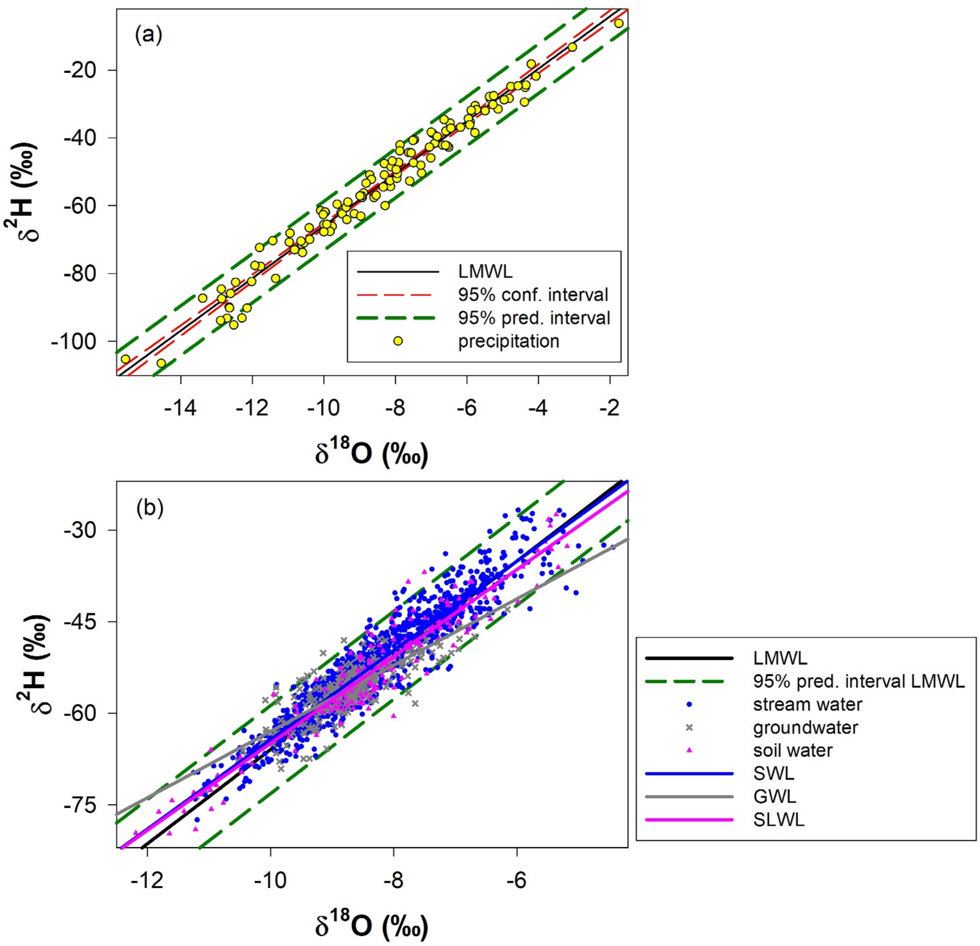

Figure 5. (a) Local meteoric water line (LMWL) and (b) δ^2H–δ^{18}O plots for stream water, groundwater and soil water in the Ressi catchment. Sample size is 116, 1,358, 248 and 161 for precipitation, stream water, groundwater and soil water, respectively. All regressions present p-values lower than 0.01.

0.42 ± 0.06‰, respectively. By the application of the amplitude ratio method, F_{yw0} values were 0.64 ± 0.06, 0.45 ± 0.07 and 0.16 ± 0.03 for stream water, soil water, and groundwater, respectively.

F_{yw} estimated based on alternative approaches are shown in Table 6. Six types of moving time windows were used to obtain the time-variable F_{ywt} and their flow-weighted averages to characterize the overall features during the observation period. The average *Ap* obtained by time-window method in different types ranged between 2.31~ ± 0.30 and 2.55 ± 0.49 for precipitation, which were similar to that obtained from the whole-period fitting method, while the average *As* ranged between 0.85 ± 0.18 and 0.99 ± 0.15, all significantly lower than that obtained by the whole-period fitting. The average goodness of fit expressed by adjusted R^2 values ranged from 0.59 to 0.65 for δ^{18}O in precipitation, which were all higher than that of whole-period fitting (0.51), while the adjusted R^2

Table 4
Parameters of δ^2H–δ^{18}O Regression for Different Water Sources in the Ressi Catchment From 2012 to 2022

Water sources	Number of samples	Abbreviation for dual isotope plot	Slope	Slope SE	Intercept	Intercept SE	R^2
Precipitation	116	LMWL	7.72	0.13	11.25	1.12	0.97
Stream water	1,358	SWL	7.31	0.07	8.82	0.59	0.89
Soil water	161	SLWL	7.12	0.18	6.27	1.54	0.90
Groundwater	248	GWL	5.43	0.24	−8.66	2.07	0.68

Note. SE is the Standard Error.

Table 5
Sen's Slopes and Relative Slopes for Short-Term (October 2012–September 2022) Monthly Isotopic Data in the Ressi Catchment (Double and Single Asterisks Mean the Results Are Significant at 0.01 and 0.05 Confidence Level, Respectively, Identified by Pre-Whitening Mann-Kendall Test)

Variable	Z value	Sen's slope	Relative slope
$\delta^{18}O$ in precipitation	2.63	0.161‰/yr**	17.9%/10yr**
$\delta^{18}O$ in stream water	14.37	0.075‰/yr*	8.7%/10yr*
$\delta^{18}O$ in soil water	2.62	0.208‰/yr**	23.9%/10yr**
$\delta^{18}O$ in groundwater	4.16	0.111‰/yr**	10.4%/10yr**

Note. Sen's slope values are reported at the annual scale.

ranged from 0.19 to 0.29 for $\delta^{18}O$ in stream water, which was much lower compared with that of whole-period fitting (0.48). The average F_{ywt} in stream water under different time-window types ranged from 0.44 ± 0.12 (2-year window with monthly step) to 0.50 ± 0.20 (1-year window with biweekly step). Taking the uncertainties into consideration, the ranges of averaged F_{ywt}(1-bw) and F_{ywt}(1-m) overlapped with that of F_{yw0} of 0.64 ± 0.06, but the average F_{ywt} was generally lower than the F_{yw0}. Slight differences in estimated F_{yw} can be observed when changing the size of time windows, and the uncertainty decreased with the increased time window width.

As proposed by Stockinger et al. (2019), a low goodness of fit (i.e., mean R^2 values lower than 0.20 for $\delta^{18}O$ in precipitation and stream water in each time window) in the fitting model is correlated with high uncertainty of estimated F_{ywt}. In the Ressi catchment, the negative relation between mean R^2 of $\delta^{18}O$ in precipitation and stream water and F_{yw} uncertainty can also be observed in all six types of time windows (as shown in Figure 8). F_{ywt} uncertainty tended to be high and fluctuated greatly when the mean R^2 was lower than 0.30 and 0.25 for 1-year and 2-year time windows, respectively, which is slightly higher compared to the threshold R^2 (0.20) reported for Wüstebach catchment in Germany (Stockinger et al., 2019). If the time windows

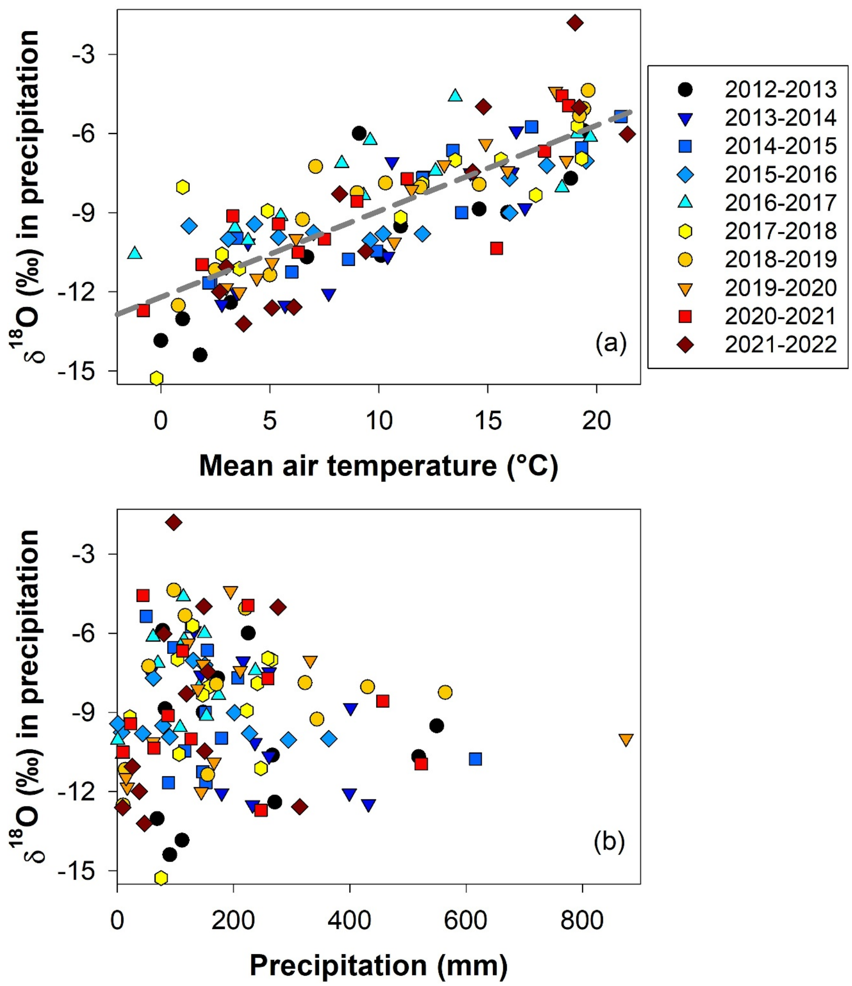

Figure 6. Relations between monthly volume-weighted $\delta^{18}O$ in precipitation and (a) monthly mean temperature and (b) monthly precipitation amount. Different colors and symbols are used for the hydrological years. The gray dashed line represents the $\delta^{18}O$-Temperature regression for the whole period. Parameters of the regressions applied to each hydrological year are reported in Table S1 of Supporting Information S1.

10.1029/2023WR036245

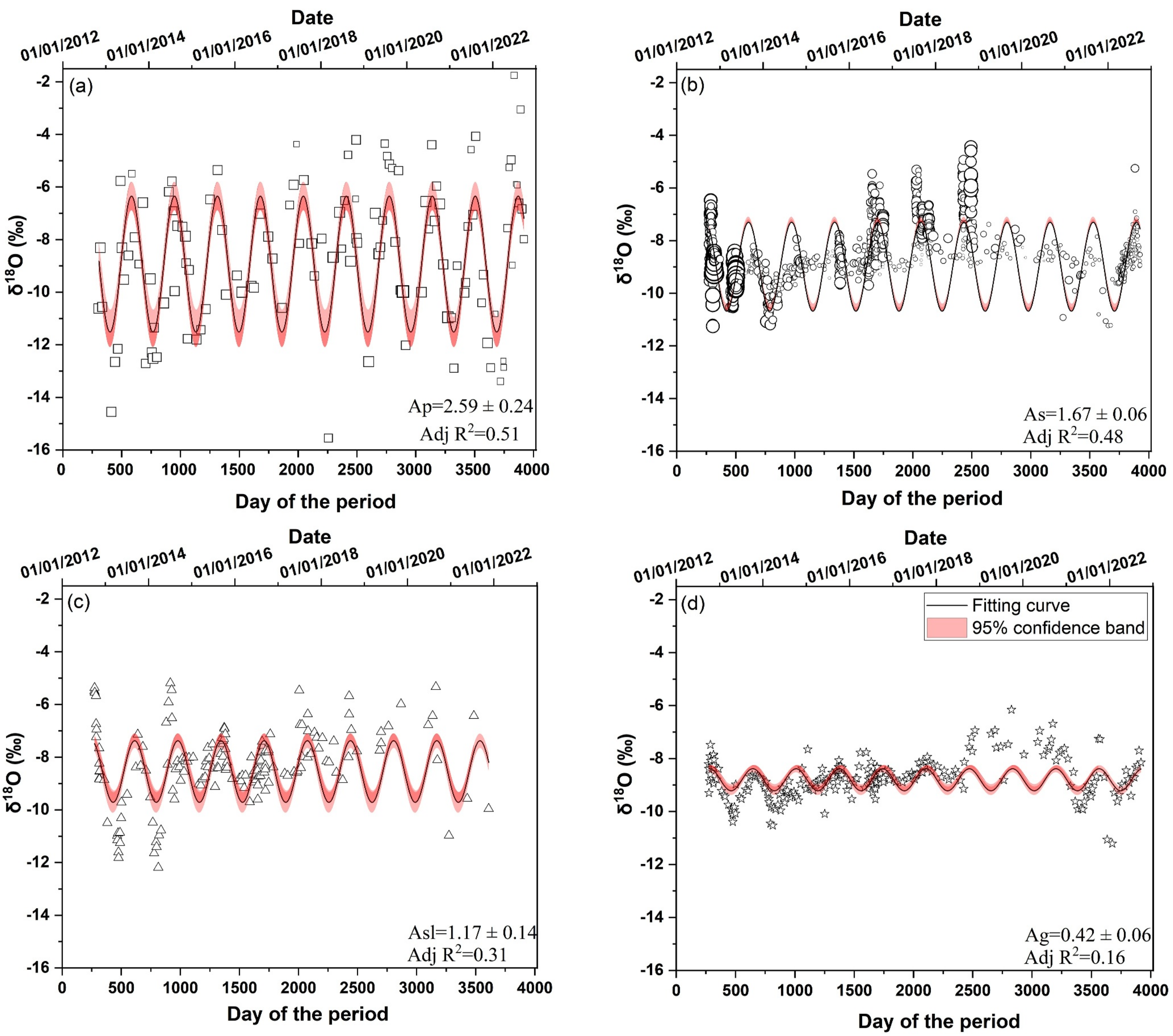

Figure 7. Fitted sine wave curve of $\delta^{18}O$ time series in (a) measured precipitation, (b) stream water, (c) soil water and (d) groundwater from October 2012 to September 2022. The size of squares and circles are proportional to the precipitation amount and discharge, respectively.

with mean R^2 values lower than the threshold were left out, the average F_{ywt}*(1-m), F_{ywt}*(1-bw), F_{ywt}*(2-m), F_{ywt}*(2-bw) obtained for the Ressi catchment would be 0.48 ± 0.16, 0.49 ± 0.16, 0.43 ± 0.10, and 0.44 ± 0.10, respectively, which were all similar to the F_{ywt} values, with slightly decreased uncertainty. To identify the possible factors controlling the difference in F_{ywt}, the relations between F_{ywt}(2-m) and F_{ywt}*(2-m) with mean discharge and cumulative precipitation amount were set up in Figure S2 of Supporting Information S1. There was a significant positive F_{ywt}(2-m)-mean discharge relation at 0.01 confidence level, but with a low R^2 (0.22). The R^2 value rose to 0.38 when F_{ywt}*(2-m) was used for the analysis (Figure S2c in Supporting Information S1). The relation was not significant between cumulative precipitation amount with both F_{ywt}(2-m) and F_{ywt}*(2-m).

The temporal trends of isotopes are considered to be a potential impact which may change the amplitudes of the fitted sine waves and lead to possibly higher uncertainties. In the Ressi catchment, significantly positive isotopic trends can be observed for different waters during the 10 hydrological years (Table 5). After using the detrending correction, the fitted *As* and *Ap* were 1.48 ± 0.05‰ and 2.47 ± 0.24‰, respectively. Notably, these values were found to be lower compared to those derived from the whole-period fitting approach, thereby affirming the

Table 6
Comparison of Estimated Ap, As and F_{yw} Based on Different Methods (Where "_avg" Means the Average Value of F_{yw} for All Time Windows or Under All Stream Discharges)

Method	*Ap* (‰)	*Adj* R^2 *(Ap)*	*As* (‰)	*Adj* R^2 *(As)*	F_{yw}
F_{yw0}	2.59 ± 0.24	0.51	1.67 ± 0.06	0.48	0.64 ± 0.06
F_{ywt}(1-bw)_avg	2.48 ± 0.48	0.63	0.85 ± 0.18	0.29	0.50 ± 0.20
F_{ywt}*(1-bw)_avg	2.62 ± 0.47	0.69	0.86 ± 0.18	0.31	0.49 ± 0.16
F_{ywt}(1-m)_avg	2.55 ± 0.49	0.65	0.86 ± 0.19	0.28	0.49 ± 0.18
F_{ywt}*(1-m)_avg	2.71 ± 0.47	0.71	0.86 ± 0.19	0.31	0.48 ± 0.16
F_{ywt}(2-bw)_avg	2.34 ± 0.36	0.60	0.88 ± 0.16	0.21	0.44 ± 0.12
F_{ywt}*(2-bw)_avg	2.56 ± 0.34	0.68	0.93 ± 0.16	0.25	0.44 ± 0.10
F_{ywt}(2-m)_avg	2.36 ± 0.37	0.60	0.87 ± 0.16	0.21	0.44 ± 0.12
F_{ywt}*(2-m)_avg	2.59 ± 0.35	0.68	0.92 ± 0.16	0.25	0.43 ± 0.10
F_{ywt}(3-bw)_avg	2.31 ± 0.30	0.59	0.99 ± 0.15	0.19	0.45 ± 0.09
F_{ywt}(3-m)_avg	2.33 ± 0.30	0.60	0.98 ± 0.15	0.19	0.45 ± 0.09
F_{ywc}	2.47 ± 0.24	0.49	1.48 ± 0.05	0.47	0.60 ± 0.06
F_{yw}(*Q*)_avg	/	/	/	/	0.67

augmented magnitude of modeled fluctuations by sinusoidal function in the presence of a discernible trend. The corrected amplitudes resulted in a F_{ywc} of 0.60 ± 0.06, which was also slightly lower than the F_{yw0} from the whole-period fitting (0.64 ± 0.06). The R^2 values of the corrected fitting curves were 0.49 and 0.47 for precipitation and stream water, respectively, which were close to those obtained by the whole-period fittings (0.51 and 0.48 for precipitation and stream water, respectively).

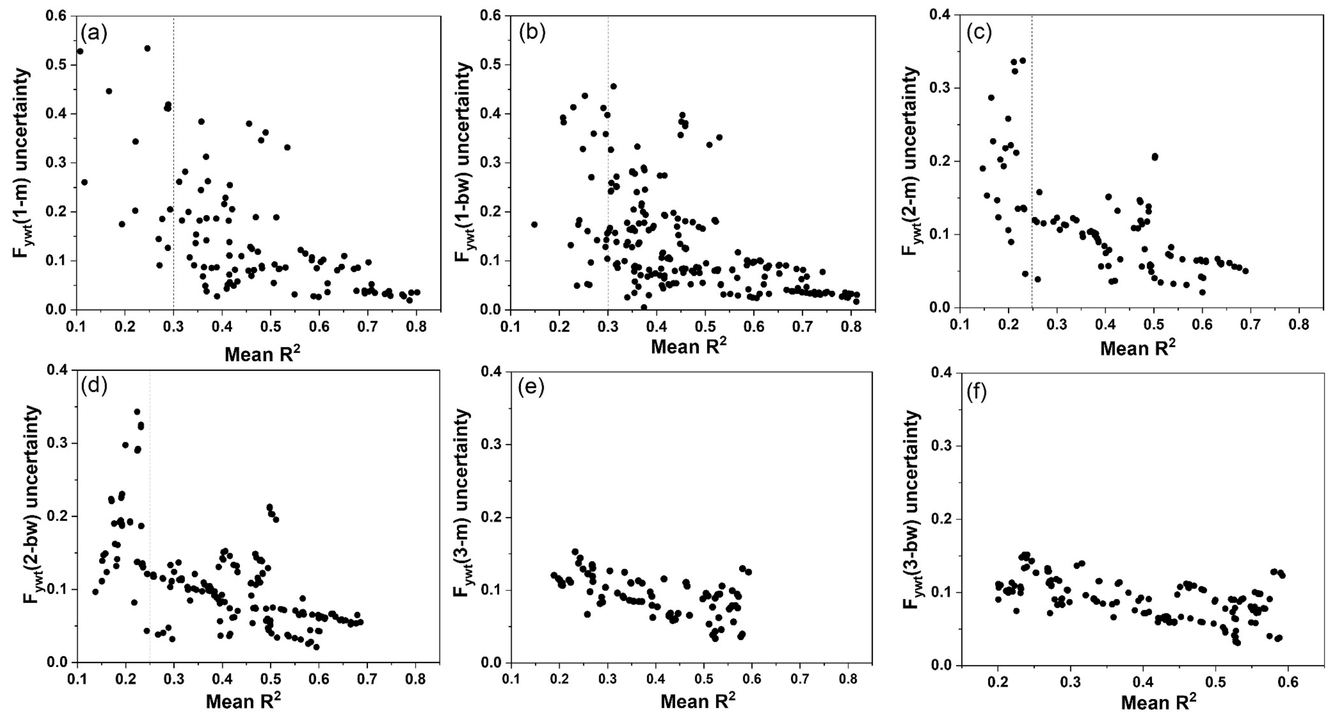

Figure 8. Relation between uncertainty of estimated F_{ywt} and mean R^2 values of fitted sine waves for precipitation and stream water for 1-year (a, b), 2-year (c, d) and 3-year (e, f) time windows with monthly and biweekly steps. The dashed line represents the mean R^2 value of 0.30 and 0.25 for 1-year and 2-year time windows, respectively.

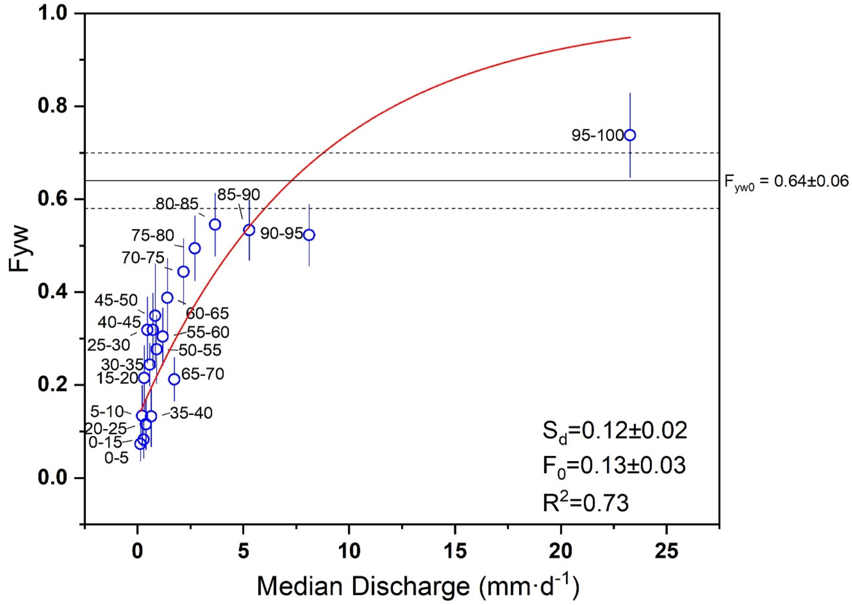

Figure 9. Relation between F_{yw} and median discharge and the fitting results using non-linear regression. Acronyms S_d and F_0 represent the discharge sensitivity metric (with a unit of Q^{-1}) and *Y*-intercept obtained by non-linear fitting of the equation. The solid black line represents the estimated F_{yw} based on the whole-period fitting, whereas the dashed lines indicate the uncertainty band.

By applying Equation 15 proposed by Gallart, von Freyberg, et al. (2020), the relation between F_{yw} and median discharge was established (Figure 9). Generally, F_{yw} showed an upward trend with the increase of the median discharge. The estimated F_{yw0} (i.e., 0.64 ± 0.06) fell near the estimated results of 80–85 (F_{yw} = 0.54 ± 0.07), 85–90 (F_{yw} = 0.53 ± 0.07), 90–95 (F_{yw} = 0.52 ± 0.07) and 95–100 (F_{yw} = 0.74 ± 0.09) discharge percentiles. The discharge sensitivity metric *Sd* was determined as 0.12 ± 0.02 through the exponential fitting. The R^2 value for the exponential fitting was 0.73, however, the regression curve fitted badly when selecting the 90–95 (estimated: 0.52 ± 0.07 vs. modeled: 0.67) and 95–100 (estimated: 0.74 ± 0.09 vs. modeled: 0.95) discharge percentile for F_{yw} estimation, leading to potential large overestimation for the top 10% high flow conditions when using the discharge-sensitive modeling. By integrating the discharge sensitivity over the continuously measured 5-min discharge records spanning the whole observation period, the modeled $F_{yw}(Q)$ was determined to vary from 0.13 to 1, with a flow-weighted average of 0.67, which was similar to the F_{yw0}.

4. Discussion

4.1. Influences of Short-Term Hydrometeorological Variations on the Isotopic Composition of Water

Based on the comparison of trends (identified by Sen's slope and relative slope) with long-term local meteorological data, it has been proved that our observation from October 2012 to September 2022 was within a period of rapid dry and warm local climatic conditions. A global-scale study reported trends in temperature, precipitation, and δ^{18}O in precipitation based on 98 long-term GNIP stations with records of more than 10 years (Wang & Chen, 2020). In Wang and Chen (2020), average Sen's slope of temperature for temperature-increasing stations was 0.0037°C/month, and that of precipitation for the precipitation-decreasing stations was −0.0372 mm/month. The monthly temperature increase and precipitation amount decrease were 0.013°C and 0.53 mm in the Ressi catchment, which were approximately 4 and more than 14 times as much as the reported large-scale averages (Wang & Chen, 2020), respectively. This reveals that our study area was experiencing fast climatic variations during the observation period. For δ^{18}O in precipitation, only 10 out of 65 global stations showed increasing rates higher than 0.0050‰/month and the maximum rate was 0.0097‰/month (Wang & Chen, 2020). In the Ressi catchment, the monthly isotopic increase in precipitation was 0.0175‰, greatly exceeding the reported increasing rate of the GNIP data set. According to the relation between δ^{18}O and temperature and their similar upward trends, the isotopic variation in precipitation could be dominated by temperatures in Ressi. Masiol et al. (2021) reported a regional-scale, long-term δ^{18}O-temperature relation based on 36 stations in northeastern Italy, which is geographically adjacent to our catchment, and found the ranges of slopes and intercepts of the regressions were 0.28~0.53‰/°C and −10~−14‰, respectively. Our results for the Ressi catchment during the 10 hydrological years (0.33 for slope and −12.20 for intercept) were included within the ranges of slope and intercepts determined by Masiol et al. (2021). Similar δ^{18}O slopes for the δ^{18}O-temperature relations were also reported in other studies, such as 0.41‰/°C for German sites (Stumpp et al., 2014), 0.31‰/°C for mid-latitude GNIP stations within 40°N–60°N (Araguas-Araguas et al., 2000) and 0.4~0.5‰/°C for three American locations (Kohn & Welker, 2005). Although our observation period was characterized by rapid climatic variations, the isotopic composition can be considered to vary in agreement with previous studies (Masiol et al., 2021; Stumpp et al., 2014). However, the R^2 value for δ^{18}O-temperature regression was 0.65, indicating that isotopic trends cannot be fully explained only by variations in temperature. The altered trajectory of air masses and variations in moisture sources represent additional potential contributors to the isotopic trends. These influences, while susceptible to being overshadowed by temperature signals, can be further substantiated through the combined δ^{18}O and d-excess analysis, as well as employing modeling techniques. Other factors, such as precipitation amount and relative humidity, are also likely to cause significant isotopic variations especially for long time spans or periods under extremely dry conditions (Eastoe & Dettman, 2016; Liu et al., 2023; Natali et al., 2023), although their influence during our short-term observation was weak (precipitation amount) or could not be assessed (relative humidity). The isotopes in all other waters also showed positive trends during the observation period, but the magnitude of isotope increase differed significantly, indicating different sensitivity in response to climatic variations.

4.2. Influence of Temporal Isotopic Trends on the F_{yw} Estimation

Jasechko et al. (2016) reported the distribution of F_{yw} in 254 global rivers spanning a large spatial range. In their study, the unweighted average, volume weighted average, and median values of F_{yw} were 0.26, 0.34 and 0.21, respectively. The estimated F_{yw0} (0.64) and F_{ywt} (0.43–0.50) in Ressi were much larger than the average and median values in the global study by Jasechko et al. (2016). The high F_{yw} is unexpected for Ressi with an average slope of 31°, due to the significant negative correlation between F_{yw} and topographic gradient of catchments (Jasechko et al., 2016). The small catchment size, short flow paths, dense vegetation coverage and the seasonal distribution of precipitation, which could accelerate the water circulation and shorten the residence time, are possible causes accounting for the high F_{yw} in Ressi, according to previous findings about the controls on F_{yw} (Ye et al., 2022; von Freyberg et al., 2018; Song et al., 2017). The strong correlation between precipitation amount and discharge, the high CV values for discharge, coupled with the congruent isotopic patterns in stream water and precipitation (Figure 4), suggests that stream water is an active hydrological component responding fast and markedly to the precipitation input (Figure 3 and Figures S1c and S1d in Supporting Information S1), thereby bolstering the observed high F_{yw}. Previous work in the same catchment also showed the high proportion of event precipitation in discharge and the fast responses of stream water to precipitation input (Gelmini et al., 2022; Penna et al., 2015; Zuecco et al., 2016).

The computed F_{yw} are not only dependent on catchment properties and hydrometeorological variables, but they are also affected by methodological factors, such as weighting methods, sampling frequency, and selected calculation period (Ceperley et al., 2020; von Freyberg et al., 2018; Gallart, Valiente, et al., 2020; Stockinger et al., 2019). It is of great importance to clarify the potential sources of uncertainty in F_{yw} estimation and thus improve the accuracy of quantification (Xia et al., 2023). The commonly used "amplitude ratio method" in F_{yw} estimation assumes that the isotopic composition of precipitation and stream water varies seasonally following a stationary sine-form curve. However, isotopic signals in waters do not fluctuate following a constant function curve in real catchments. A whole-period sinusoidal fitting on multi-year records will oversimplify the shapes of interannual isotopic signals, leading to unreliable results in F_{yw} estimations. As proved by Stockinger et al. (2019), the interannual variability in isotopic fluctuation results in increased uncertainty of F_{yw} estimation. Compared with the whole-period fitting, mean F_{yw} from moving time windows was recommended because it ensures the variability and uncertainty within the entire range to be considered. In the Ressi catchment, six types of time windows were employed to calculate the time-variable F_{yw}. As shown in Table 6, the average F_{ywt} values by different time windows were slightly different and the length of timesteps had a negligible impact on average F_{ywt}. The uncertainty decreased significantly with the increased size of time windows, indicating that the results could be more robust when using longer data series for sinusoidal fitting, which may help obtain more information on isotopic variation. A great difference in the goodness of fit was detected between the time-window method and the whole-period fitting method. The R^2 values was higher for $\delta^{18}O$ in precipitation when using time-window method than using the whole-period fitting. This is likely attributable to the representation of distinctive isotopic periodicities within each specific period (1–3 years) by individual sinusoidal curves. However, the R^2 values were much lower for $\delta^{18}O$ in stream water when using time-window method. This could be attributed to the different density of samples and the varying proportions of samples collected under different flow conditions during each calculation period. In contrast to the findings reported by Stockinger et al. (2019), which observed a close agreement between F_{yw} values derived from averaged time windows and those from whole-period fitting, our study in Ressi revealed a markedly higher F_{yw0} compared to all F_{ywt} (as well as F_{ywt}*) values. The *Ap* values observed by the two methods were not quite different, while the average *As* values were much smaller when obtained by the time-window method. Previous studies showed that *As* was closely related to discharge and sampling design (von Freyberg et al., 2018; Gallart, Valiente, et al., 2020; Trinh et al., 2020). Therefore, the pronounced *As* difference reflected the influence of data and methods on the fittings of isotopic signals in stream water in the Ressi catchment. On the one hand, the difference could be partly attributed to the irregular sampling campaigns carried out during the various years. When using the least square regression method, data-intensive periods imposed a greater influence on the fitting parameters than periods with sparse data, although discharge was used as weights. For example, the highest sample counts were recorded during the hydrological years October 2012–September 2013 (355 samples) and October 2016–September 2017 (286 samples) among the observation period, with corresponding annual F_{yw} values of 0.69 and 1, respectively, which would contribute greatly to the elevated overall F_{yw}. On the other hand, another possible cause for the difference in F_{yw} could be the isotopic trends. As illustrated above, the isotopic composition of waters in Ressi showed significant upward trends (Table 5). The Sen's slopes were high for $\delta^{18}O$ in precipitation (0.161‰/yr) and stream water (0.075‰/yr), in comparison with results of other studies. The diminished *As* and *Ap* values subsequent to the detrending correction indicated that the presence of positive trends may exacerbate the fitting by a fixed periodic function, regardless of whether this trend is entirely attributable to climate variations. Although the F_{ywc} (0.60 ± 0.06) was only slightly lower than the F_{yw0} (0.64 ± 0.06), it is crucial to recognize the overestimation resulting from isotopic trends as a potential source of uncertainty in F_{yw} estimation utilizing sinusoidal functions. In future studies, it is essential to delve deeper into the effects of isotopic trends across various scenarios (e.g., positive or negative trends, and differing magnitudes between precipitation and other waters) on the F_{yw} results and new methods considering the trends should be developed for more accurate F_{yw} estimation.

The high discharge sensitivity and the significant positive relations between mean discharge and F_{ywt}(2-m) and F_{ywt}*(2-m) (Figure S2 in Supporting Information S1) indicated that the discharge is a key factor influencing the F_{yw} results. Therefore, another source of uncertainty for both whole-period fitting and time-window method is that the captured discharge with isotope sampling (abbreviated as "isotopic discharge") cannot represent the real discharge variation in the catchment, considering the high discharge sensitivity of F_{yw}. For example, when employing the 2-year time windows with monthly timesteps, the median isotopic discharge within each time window ranged from 0.84 to 42.33 mm/d, with an average of 9.45 mm/d. However, the median 5-min discharge within each time window varied between 0.52 and 1.86 mm/d, with an average of 0.94 mm/d. A *t*-test showed that the two median discharge series (the comparison is shown in Figure S3 of Supporting Information S1) had a significant difference ($p < 0.01$). Therefore, the real discharge variability cannot be completely reflected by the isotopic discharge and thus the estimated F_{ywt}(2-m) may be faced with uncertainty.

The F_{yw} modeled based on the discharge sensitivity metrics and flow duration curve is an effective new approach showing potential to obtain a more accurate F_{yw}, which was reported to perform well in some catchments (Gallart, Valiente, et al., 2020). However, the fitting result by the non-linear curve was not so satisfactory in our catchment, especially for the F_{yw} estimated under 0–5 and 5–10 discharge percentiles. As shown in Figure 9, the F_{yw} may depend more on the samples collected during high flow periods than those collected during baseflow, owing to the considerable variability in flow regime and the high discharge sensitivity of F_{yw}, which resulted in the rapid circulation of a significant portion of the young water mass during transient high-flow events. Considering the high discharge sensitivity of the Ressi catchment and incorporation of discharge as weights in dynamic F_{yw} modeling, the average $F_{yw}(Q)$ of 0.67 may be faced with non-negligible overestimation. Furthermore, the relative uncertainty of estimated F_{yw} under low flow condition was considerable, reaching 51%, 49% and 49% for the discharge percentiles of 0–5, 5–10 and 10–15, respectively. Such heightened uncertainty further diminished the robustness of the fitted relation between F_{yw} and median discharge. This is likely due to the low temporal resolution of isotopic data, as we collected isotopic data for stream water at approximate monthly scale and only collected hourly or 10-min data in very limited high-flow events, far below the 30-min to weekly data applied in the study by Gallart, Valiente, et al. (2020). Stockinger and Stumpp (2024) recently reported a failure in using the discharge-sensitive method in their case, with monthly resolution stream isotopic data. Therefore, the paucity of isotopic input data is likely to constitute a constraint when employing the discharge-sensitive method. To achieve an accurate modeling of discharge-sensitive F_{yw}, the sampling strategy should prioritize a comprehensive capture of isotopic data under high-flow conditions and increase sampling frequency during baseflow periods (at least to a weekly resolution).

5. Conclusions

Based on hydrometeorological observations and isotopic data collected in the Ressi experimental catchment during 10 hydrological years from October 2012 to September 2022, this study reports new evidence on the effects of short-term climatic variations and sampling strategies on the isotopic composition of water sources and the young water fraction (F_{yw}) estimation.

The monthly average air temperature increase and precipitation decrease, expressed by the Sen's slope, were both much higher than the previously reported local and global rates, indicating that in the last 10 years the Ressi catchment underwent climate variability with rapid warming and drying trends. A marked trend of isotopic enrichment was observed in all waters, and air temperature was a potential factor driving the isotopic variation in precipitation.

By employing the amplitude ratio method, F_{yw} was estimated to be 0.64 ± 0.06, 0.45 ± 0.07 and 0.16 ± 0.03 for stream water, soil water, and shallow groundwater, respectively. For stream water, F_{ywt} of the averaged results from moving time windows ranged from 0.43 to 0.50, which were lower than the F_{yw0} estimated by fitting the whole-period data. Such difference can be derived from the uneven temporal data distribution in the whole-period fitting and the potential impact from isotopic trends. The comparison between F_{yw0} and F_{ywc} obtained after the detrending correction verified the significant impact of isotopic trends on the fitted isotopic amplitudes which led to a slight F_{yw0} overestimation. Based on the discharge sensitivity metrics obtained from the median discharge-F_{yw} relation, continuous $F_{yw}(Q)$ was modeled with an average of 0.67. The bad nonlinear fit for high-flow condition and the high F_{yw} uncertainty for baseflow conditions implied a possible overestimation in average $F_{yw}(Q)$ and underscored the necessity for enhanced data resolution during both high-flow and baseflow periods to ensure accurate results by this alternative approach.

Our results provide currently missing information on the importance of taking interannual isotopic trends into consideration when estimating F_{yw} based on multiple years, especially under fast climatic variations. The adoption of average values obtained by moving time windows and the discharge sensitivity-based F_{yw} modeling can represent effective methods to mitigate the limitations of fitting multi-year isotopic data with fixed functions in F_{yw} estimation. However, the relations between the distribution of data and estimated F_{yw} should be further explored when using the moving time windows, to better optimize the sampling effort aimed to the F_{yw} estimation. Further research should be performed to develop better models reflecting the natural trends of isotopic variation.

Conflict of Interest

The authors declare no conflicts of interest relevant to this study.

Data Availability Statement

Hydrometeorological and isotopic data collected in the Ressi experimental catchment are available from the Open Science Framework and are shared under a Creative Commons Attribution 4.0 International license (Zuecco & Marchina, 2021).

Acknowledgments

Research in the Ressi catchment was supported by the project "Giovani Studiosi-Ricerche di carattere innovative e di eccellenza proposte da giovani non strutturati, decreto rettorale n. 800–2011, 23/03/2011, University of Padova", the grant "Bando 2014 per il finanziamento di attrezzature scientifiche finalizzate alla ricerca" (University of Padova), the project "Ecohydrological Dynamics and Water Pathways in Forested Catchments" (Bando Starting Grants 2015; Fondazione Cassa di Risparmio di Padova e Rovigo), the project "SILVA-Water fluxes between soil, vegetation and atmosphere: a comparative analysis in two Italian forested catchments" (funded by Premio Florisa Melone 2018; assigned by the Italian Hydrological Society), and the Italian MIUR Project (PRIN 2017) "WATer mixing in the critical ZONe: observations and predictions under environmental changes-WATZON" (code: 2017SL7ABC, national coordinator: Marco Borga). This study was also carried out within the Agritech National Research Center and received funding from the European Union Next-Generation EU (PIANO NAZIONALE DI RIPRESA E RESILIENZA (PNRR)—MISSIONE 4 COMPONENTE 2, INVESTIMENTO 1.4 —D.D. 1032 17/06/2022, CN00000022), and within the RETURN Extended Partnership and received funding from the European UnionNext-Generation EU (National Recovery and Resilience Plan—NRRP, Mission 4, Component 2, Investment 1.3—D.D. 1243 2/8/2022, PE0000005). This manuscript reflects only the authors' views and opinions; neither the European Union nor the European Commission can be considered responsible for them. The authors thank the associate editor (Christine Stumpp), Francesc Gallart and two anonymous reviewers for the useful comments which helped to improve the manuscript.

References

Araguas-Araguas, L., Froehlich, K., & Rozanski, K. (2000). Deuterium and oxygen-18 isotope composition of precipitation and atmospheric moisture. *Hydrological Processes*, *14*(8), 1341–1355. https://doi.org/10.1002/1099-1085(20000615)14:8<1341::aid-hyp983>3.0.co;2-z

Bansah, S., & Ali, G. (2019). Streamwater ages in nested, seasonally cold Canadian watersheds. *Hydrological Processes*, *33*(4), 495–511. https://doi.org/10.1002/hyp.13373

Barua, S., Cartwright, I., Dresel, P. E., Morgenstern, U., McDonnell, J. J., & Daly, E. (2022). Sources and mean transit times of intermittent streamflow in semi-arid headwater catchments. *Journal of Hydrology*, *604*, 127208. https://doi.org/10.1016/j.jhydrol.2021.127208

Benettin, P., Rodriguez, N. B., Sprenger, M., Kim, M., Klaus, J., Harman, C. J., et al. (2022). Transit time estimation in catchments: Recent developments and future directions. *Water Resources Research*, *58*(11), e2022WR033096. https://doi.org/10.1029/2022WR033096

Burt, E. I., Coayla Rimachi, D. H., Ccahuana Quispe, A. J., Atwood, A., & West, A. J. (2023). Isotope-derived young water fractions in streamflow across the tropical Andes Mountains and Amazon floodplain. *Hydrology and Earth System Sciences*, *27*(15), 2883–2898. https://doi.org/10.5194/hess-27-2883-2023

Ceperley, N., Zuecco, G., Beria, H., Carturan, L., Michelon, A., Penna, D., et al. (2020). Seasonal snow cover decreases young water fractions in high Alpine catchments. *Hydrological Processes*, *34*(25), 4794–4813. https://doi.org/10.1002/hyp.13937

Cox, D. R., & Stuart, A. (1955). Some quick sign tests for trend in location and dispersion. *Biometrika*, *42*(1/2), 80. https://doi.org/10.2307/2333424

Craig, H. (1961). Isotopic variations in meteoric waters. *Science*, *133*(346), 1702–1703. https://doi.org/10.1126/science.133.3465.1702

Dansgaard, W. (1964). Stable isotopes in precipitation. *Tellus*, *16*(4), 436–468. https://doi.org/10.3402/tellusa.v16i4.8993

Dutton, A., Wilkinson, B. H., Welker, J. M., Bowen, G. J., & Lohmann, K. C. (2005). Spatial distribution and seasonal variation in $^{18}O/^{16}O$ of modern precipitation and river water across the conterminous USA. *Hydrological Processes*, *19*(20), 4121–4146. https://doi.org/10.1002/hyp.5876

Eastoe, C. J., & Dettman, D. L. (2016). Isotope amount effects in hydrologic and climate reconstructions of monsoon climates: Implications of some long-term data sets for precipitation. *Chemical Geology*, *430*, 78–89. https://doi.org/10.1016/j.chemgeo.2016.03.022

Gallart, F., Valiente, M., Llorens, P., Cayuela, C., Sprenger, M., & Latron, J. (2020). Investigating young water fractions in a small Mediterranean mountain catchment: Both precipitation forcing and sampling frequency matter. *Hydrological Processes*, *34*(17), 3618–3634. https://doi.org/10.1002/hyp.13806

Gallart, F., von Freyberg, J., Valiente, M., Kirchner, J. W., Llorens, P., & Latron, J. (2020). Technical note: An improved discharge sensitivity metric for young water fractions. *Hydrology and Earth System Sciences*, *24*(3), 1101–1107. https://doi.org/10.5194/hess-24-1101-2020

Gelmini, Y., Zuecco, G., Zaramella, M., Penna, D., & Borga, M. (2022). Hysteresis in streamflow-water table relation provides a new classification system of rainfall-runoff events. *Hydrological Processes*, *36*(9), e14685. https://doi.org/10.1002/hyp.14685

Gentile, A., Canone, D., Ceperley, N., Gisolo, D., Previati, M., Zuecco, G., et al. (2023). Towards a conceptualization of the hydrological processes behind changes of young water fraction with elevation: A focus on mountainous alpine catchments. *Hydrology and Earth System Sciences*, *27*(12), 2301–2323. https://doi.org/10.5194/hess-27-2301-2023

Hamed, K. H., & Ramachandra Rao, A. (1998). A modified Mann-Kendall trend test for autocorrelated data. *Journal of Hydrology*, *204*(1–4), 182–196. https://doi.org/10.1016/S0022-1694(97)00125-X

Jasechko, S., Kirchner, J. W., Welker, J. M., & McDonnell, J. J. (2016). Substantial proportion of global streamflow less than three months old. *Nature Geoscience*, *9*(2), 126–129. https://doi.org/10.1038/ngeo2636

Kahya, E., & Kalayci, S. (2004). Trend analysis of streamflow in Turkey. *Journal of Hydrology*, *289*(1–4), 128–144. https://doi.org/10.1016/j.jhydrol.2003.11.006

Kirchner, J. W. (2016). Aggregation in environmental systems-Part 1: Seasonal tracer cycles quantify young water fractions, but not mean transit times, in spatially heterogeneous catchments. *Hydrology and Earth System Sciences*, *20*(1), 279–297. https://doi.org/10.5194/hess-20-279-2016

Kohn, M. J., & Welker, J. M. (2005). On the temperature correlation of $\delta^{18}O$ in modern precipitation. *Earth and Planetary Science Letters*, *231*(1–2), 87–96. https://doi.org/10.1016/j.epsl.2004.12.004

Liu, Z., Zhang, X., Xiao, Z., He, X., Rao, Z., & Guan, H. (2023). The relations between summer droughts/floods and oxygen isotope composition of precipitation in the Dongting Lake basin. *International Journal of Climatology*, *43*(8), 3590–3604. https://doi.org/10.1002/joc.8047

Marchina, C., Zuecco, G., Chiogna, G., Bianchini, G., Carturan, L., Comiti, F., et al. (2020). Alternative methods to determine the δ^2H–$\delta^{18}O$ relationship: An application to different water types. *Journal of Hydrology*, *587*, 124951. https://doi.org/10.1016/j.jhydrol.2020.124951

Masiol, M., Zannoni, D., Stenni, B., Dreossi, G., Zini, L., Calligaris, C., et al. (2021). Spatial distribution and interannual trends of $\delta^{18}O$, δ^2H, and deuterium excess in precipitation across North-Eastern Italy. *Journal of Hydrology*, *598*, 125749. https://doi.org/10.1016/j.jhydrol.2020.125749

Natali, S., Doveri, M., Franceschi, L., Giannecchini, R., Luppichini, M., Menichini, M., & Zanchetta, G. (2023). Moisture sources and climatic effects controlling precipitation stable isotope composition in a western Mediterranean island (Pianosa, Italy). *Atmospheric Research*, *294*, 106987. https://doi.org/10.1016/j.atmosres.2023.106987

Orlowski, N., Rinderer, M., Dubbert, M., Ceperley, N., Hrachowitz, M., Gessler, A., et al. (2023). Challenges in studying water fluxes within the soil-plant-atmosphere continuum: A tracer-based perspective on pathways to progress. *Science of the Total Environment*, *881*, 163510. https://doi.org/10.1016/j.scitotenv.2023.163510

Penna, D. (2024). A recipe for why and how to set up and sustain an experimental catchment. *Hydrological Processes*, *38*(5), e15163. https://doi.org/10.1002/hyp.15163

Penna, D., Hopp, L., Scandellari, F., Allen, S. T., Benettin, P., Beyer, M., et al. (2018). Ideas and perspectives: Tracing terrestrial ecosystem water fluxes using hydrogen and oxygen stable isotopes—challenges and opportunities from an interdisciplinary perspective. *Biogeosciences*, *15*(21), 6399–6415. https://doi.org/10.5194/bg-15-6399-2018

Penna, D., Stenni, B., Šanda, M., Wrede, S., Bogaard, T. A., Michelini, M., et al. (2012). Technical note: Evaluation of between-sample memory effects in the analysis of δ^2H and $\delta^{18}O$ of water samples measured by laser spectroscopes. *Hydrology and Earth System Sciences*, *16*(10), 3925–3933. https://doi.org/10.5194/hess-16-3925-2012

Penna, D., & van Meerveld, H. J. (Ilja). (2019). Spatial variability in the isotopic composition of water in small catchments and its effect on hydrograph separation. *WIREs Water*, *6*(5), e1367. https://doi.org/10.1002/wat2.1367

Penna, D., van Meerveld, H. J., Oliviero, O., Zuecco, G., Assendelft, R. S., Dalla Fontana, G., & Borga, M. (2015). Seasonal changes in runoff generation in a small forested mountain catchment. *Hydrological Processes*, *29*(8), 2027–2042. https://doi.org/10.1002/hyp.10347

Rank, D., Papesch, W., Heiss, G., & Tesch, R. (2012). Environmental isotope ratios of river water in the Danube basin. In *Monitoring Isotopes in Rivers: Creation of the Global Network of Isotopes in Rivers (GNIR)* (pp. 13–40). IAEA.

Reckerth, A., Stichler, W., Schmidt, A., & Stumpp, C. (2017). Long-term data set analysis of stable isotopic composition in German rivers. *Journal of Hydrology*, *552*, 718–731. https://doi.org/10.1016/j.jhydrol.2017.07.022

Rodgers, P., Soulsby, C., & Waldron, S. (2005). Stable isotope tracers as diagnostic tools in upscaling flow path understanding and residence time estimates in a mountainous mesoscale catchment. *Hydrological Processes*, *19*(11), 2291–2307. https://doi.org/10.1002/hyp.5677

Rozanski, K., Araguãs-Araguãs, L., & Gonfiantini, R. (1992). Relation between long-term trends of oxygen-18 isotope composition of precipitation and climate. *Science*, *258*(5084), 981–985. https://doi.org/10.1126/science.258.5084.981

Sen, P. K. (1968). Estimates of the regression coefficient based on Kendall's Tau. *Journal of the American Statistical Association*, *63*(324), 1379–1389. https://doi.org/10.1080/01621459.1968.10480934

Song, C., Wang, G., Liu, G., Mao, T., Sun, X., & Chen, X. (2017). Stable isotope variations of precipitation and streamflow reveal the young water fraction of a permafrost watershed. *Hydrological Processes*, *31*(4), 935–947. https://doi.org/10.1002/hyp.11077

Soulsby, C., Tetzlaff, D., Rodgers, P., Dunn, S., & Waldron, S. (2006). Runoff processes, stream water residence times and controlling landscape characteristics in a mesoscale catchment: An initial evaluation. *Journal of Hydrology*, *325*(1–4), 197–221. https://doi.org/10.1016/j.jhydrol.2005.10.024

Sprenger, M., Stumpp, C., Weiler, M., Aeschbach, W., Allen, S. T., Benettin, P., et al. (2019). The demographics of water: A review of water ages in the critical zone. *Reviews of Geophysics*, *57*(3), 800–834. https://doi.org/10.1029/2018RG000633

Stockinger, M. P., Bogena, H. R., Lücke, A., Stumpp, C., & Vereecken, H. (2019). Time variability and uncertainty in the fraction of young water in a small headwater catchment. *Hydrology and Earth System Sciences*, *23*(10), 4333–4347. https://doi.org/10.5194/hess-23-4333-2019

Stockinger, M. P., & Stumpp, C. (2024). Lessons learned from the spatiotemporal analysis of long-term and time-variable young water fractions of large central European river basins. *Hydrological Processes*, *38*(2), e15038. https://doi.org/10.1002/hyp.15038

Stumpp, C., Klaus, J., & Stichler, W. (2014). Analysis of long-term stable isotopic composition in German precipitation. *Journal of Hydrology*, *517*, 351–361. https://doi.org/10.1016/j.jhydrol.2014.05.034

Trinh, A. D., Do, T. N., Panizzo, V. N., McGowan, S., & Leng, M. J. (2020). Using stable isotopes to estimate young water fractions in a heavily regulated, tropical lowland river basin. *Hydrological Processes*, *34*(22), 4239–4250. https://doi.org/10.1002/hyp.13878

von Freyberg, J., Allen, S. T., Seeger, S., Weiler, M., & Kirchner, J. W. (2018). Sensitivity of young water fractions to hydro-climatic forcing and landscape properties across 22 Swiss catchments. *Hydrology and Earth System Sciences*, *22*(7), 3841–3861. https://doi.org/10.5194/hess-22-3841-2018

Vystavna, Y., Matiatos, I., & Wassenaar, L. I. (2021). Temperature and precipitation effects on the isotopic composition of global precipitation reveal long-term climate dynamics. *Scientific Reports*, *11*(1), 18503. https://doi.org/10.1038/s41598-021-98094-6

Wang, T., & Chen, J. (2020). Long-term trend of precipitation stable isotopic compositions under global warming conditions. *Journal of Radioanalytical and Nuclear Chemistry*, *325*(2), 557–565. https://doi.org/10.1007/s10967-020-07246-x

Xia, C., Liu, G., Zhou, J., Meng, Y., Chen, K., Gu, P., et al. (2021). Revealing the impact of water conservancy projects and urbanization on hydrological cycle based on the distribution of hydrogen and oxygen isotopes in water. *Environmental Science and Pollution Research*, *28*(30), 40160–40177. https://doi.org/10.1007/s11356-020-11647-6

Xia, C., Zuecco, G., Chen, K., Liu, L., Zhang, Z., & Luo, J. (2023). The estimation of young water fraction based on isotopic signals: Challenges and recommendations. *Frontiers in Ecology and Evolution*, *11*, 1114259. https://doi.org/10.3389/fevo.2023.1114259

Ye, S., Liu, L., Chen, X., Li, P., Xu, G., & Ran, Q. (2022). The variability of stable water isotopes and the young water fraction in a mountainous catchment. *CLEAN – Soil, Air, Water*, *50*(7), 2100337. https://doi.org/10.1002/clen.202100337

Yue, S., Pilon, P., & Cavadias, G. (2002). Power of the Mann-Kendall and Spearman's rho tests for detecting monotonic trends in hydrological series. *Journal of Hydrology*, *259*(1–4), 254–271. https://doi.org/10.1016/S0022-1694(01)00594-7

Yue, S., & Wang, C. Y. (2002). Applicability of prewhitening to eliminate the influence of serial correlation on the Mann-Kendall test. *Water Resources Research*, *38*(6). https://doi.org/10.1029/2001wr000861

Zhang, M., & Wang, S. (2016). A review of precipitation isotope studies in China: Basic pattern and hydrological process. *Journal of Geographical Sciences*, *26*(7), 921–938. https://doi.org/10.1007/s11442-016-1307-y

Zuecco, G., & Marchina, C. (2021). Hydrological data from Ressi experimental catchment (Italy). https://doi.org/10.17605/OSF.IO/N24DG

Zuecco, G., Marchina, C., Gelmini, Y., Amin, A., van Meerveld, H. J., Penna, D., & Borga, M. (2021). Ressi experimental catchment: Eco-hydrological research in the Italian pre-Alps. *Hydrological Processes*, *35*(3), e14095. https://doi.org/10.1002/hyp.14095

Zuecco, G., Penna, D., Borga, M., & van Meerveld, H. J. (2016). A versatile index to characterize hysteresis between hydrological variables at the runoff event timescale. *Hydrological Processes*, *30*(9), 1449–1466. https://doi.org/10.1002/hyp.10681

Zwiers, F. W., & Von Storch, H. (1995). Taking serial correlation into account in tests of the mean. *Journal of Climate*, *8*(2), 336–351. https://doi.org/10.1175/1520-0442(1995)008<0336:TSCIAI>2.0.CO;2